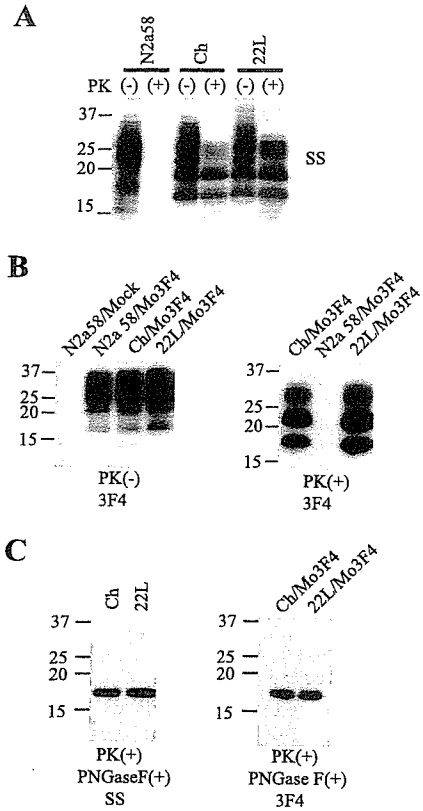

FIG. 1. Formation of Mo3F4-derived PrP^{Sc} in Ch-N2a58 and 22L-N2a58 cells. (A) Western blot using polyclonal anti-PrP antibody SS in N2a58, Ch-N2a58 (Ch), and 22L-N2a58 (22L) cells without (−) or with (+) PK treatment. (B) Expression levels of Mo3F4 PrP (left panel) and detection of Mo3F4-derived PrP^{Sc} (right panel) were measured by Western blot using monoclonal antibody 3F4. Mock, untransfected cells. (C) After consecutive treatments of PK and PNGase F, untransfected (left panel) and Mo3F4 PrP-transfected cells (right panel) were analyzed by Western blotting using SS and 3F4 antibodies, respectively. Molecular mass markers are indicated in kilodaltons on the left side of each panel.

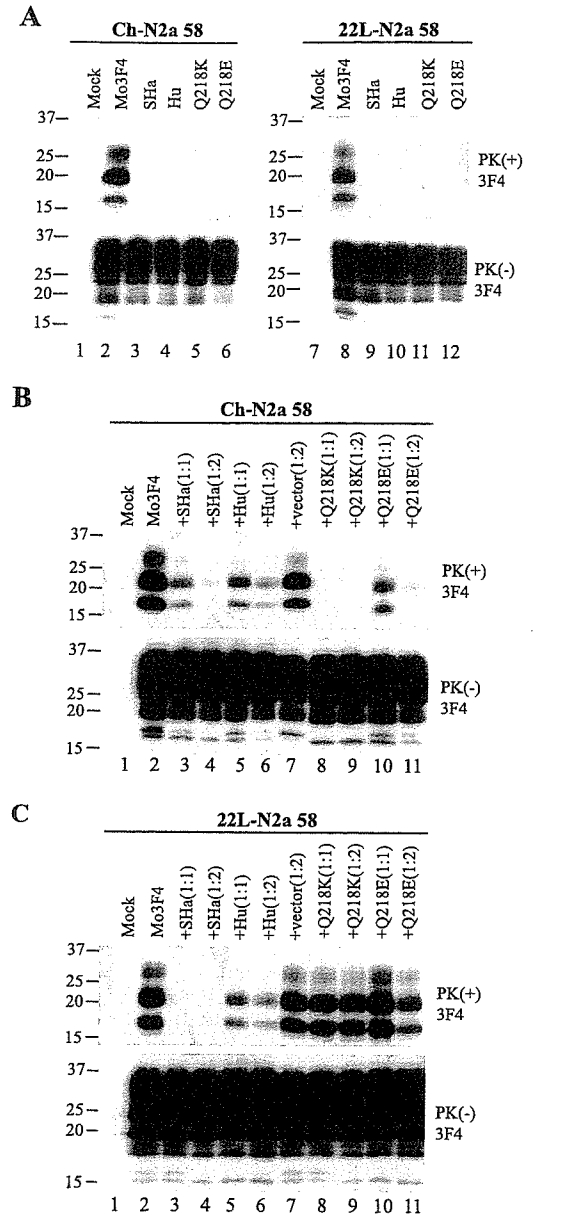

FIG. 2. Strain-dependent inhibitory effect of Q218K mutation on PrP^{Sc} formation of wild-type Mo3F4. (A) Conversion to 3F4-positive PrP^{Sc} (upper panels) and expression of Mo3F4, SHa, Hu, Q218K, and Q218E (lower panels) were measured by Western blot using 3F4 antibody. The 3F4 epitope was present in all these constructs. (B and C) The inhibitory effect of the constructs was determined by cotransfection with Mo3F4 in the DNA ratio of 1:1 or 1:2. The blots were probed with 3F4 antibody. Mock, untransfected cells; +vector(1:2), cotransfection of Mo3F4 and pcDNA3.1(+) at a 1:2 ratio.

N2a58 cells, we first examined the PrP^{Sc} formation of two heterologous PrPs, Syrian hamster (SHa) and human (Hu) PrPs, and two Mo3F4 mutated PrPs with a single amino acid substitution at codon 218, Q218K and Q218E, in the infected cells transfected with the corresponding expression vectors. The 3F4 antibody detected SHa, Hu, and Mo3F4 mutated PrPs expressed in Ch-N2a58 and 22L-N2a58 cells at a level similar to that of wild-type Mo3F4 PrP (Fig. 2A, lower panels). SHa, Hu, Q218K, and Q218E PrP did not convert to PrP^{Sc} in Ch-N2a58 (Fig. 2A, upper panel, lanes 3 to 6) and 22L-N2a58 (Fig. 2A, upper panel, lanes 9 to 12) cells.

To evaluate the inhibitory effect of these heterologous and mutated PrPs, each expression vector was cotransfected with that of Mo3F4 PrP at a DNA ratio of 1:1 or 1:2. As seen previously (26), in Ch-N2a58 cells, Q218K PrP completely inhibited the accumulation of PrP^{Sc} derived from Mo3F4 PrP even at a DNA ratio of 1:1 (Fig. 2B, upper panel, lanes 8 and 9). SHa, Hu, and Q218E PrP also revealed a dose-dependent inhibitory effect but to a lesser extent (Fig. 2B, upper panel, lanes 3 to 6, 10, and 11). In remarkable contrast, in 22L-N2a58 cells, Q218K PrP had little effect on Mo3F4 PrP^{Sc} accumulation (Fig. 2C, upper panel, lanes 8 and 9). The inhibitory effect of Q218E PrP in 22L-N2a58 cells was also very weak (Fig. 2C, upper panel, lanes 10 and 11). Conversely, SHa PrP inhibited Mo3F4-derived PrP^{Sc} formation to a greater extent in 22L-N2a58 cells than in Ch-N2a58 cells (Fig. 2C, upper panel, lanes 3 and 4). These results were reproduced in three independent experiments (Table 1). These data suggest that the inhibition

TABLE 1. Summary of results

Mutations	Chandler		22L	
	Conversion[a]	Inhibition[b]	Conversion[a]	Inhibition[b]
SHa	−	+	−	2+
Hu	−	+	−	+
Q90R	+	NA	+	NA
Q97R	−	2+	−	2+
Q159R	+	NA	+	NA
Q167R	−	2+	−	+
Q171R	−	2+	−	2+
Q185R	+	NA	−	2+
Q185K	2+	NA	−	2+
Q185H	+	NA	+/−	+
Q185E	−	+	−	+/−
Q185L	+/−	+	+/−	+
Q211R	+	NA	+	NA
Q216R	−	+	−	2+
Q218R	−	2+	+	NA
Q218K	−	2+	−	−
Q218H	−	2+	+	NA
Q218E	−	+	+/−	−
Q218L	+/−	+	+	NA
Q222R	+	NA	+	NA

[a] PrP^{Sc} formation of each 3F4-positive construct was quantified by densitometric analysis. The percent conversion of Mo3F4 was assigned as 100%, and the relative scores compared with Mo3F4 are shown. 2+ indicates >200%; + indicates 50 to 200%; +/− indicates 10 to 50%; − indicates <10%. Each value represents the mean of two or three replicates.

[b] Relative inhibitory effect on PrP^{Sc} formation of conversion-defective mutated PrPs was assessed. 2+ indicates >80% inhibition of Mo3F4 PrP^{Sc} formation (in the DNA ratio of 1:1); + indicates 50 to 80% inhibition (1:1); +/− indicates <50% inhibition (1:1) and >50% inhibition (1:2); − indicates <50% inhibition (1:1 and 1:2). Each value represents the mean of two or three replicates. NA, not applicable.

of PrP^{Sc} formation by some of these PrP molecules, especially Q218K, is strain specific.

Q185R PrP converts to PrP^{Sc} in Ch-N2a58 but not 22L-N2a58 cells. To further analyze the strain-specific effect of PrP mutations on PrP^{Sc} formation in Ch-N2a58 and 22L-N2a58 cells, we generated nine 3F4-positive mutated PrPs with a single arginine substitution for each glutamine residue in the C-terminal half and examined their conversion efficiencies in the infected cells (see Fig. 6). The Q90R, Q159R, Q211R, and Q222R PrPs readily converted to PrP^{Sc} in Ch-N2a58 and 22L-N2a58 cells (Fig. 3A, upper panels), whereas the Q97R, Q167R, Q171R, and Q216R PrPs failed to convert in both cell lines (Fig. 3A, upper panels). These conversion-defective mutated PrPs potently inhibited the accumulation of wild-type Mo3F4-derived PrP^{Sc} in both cell lines (Fig. 3B, upper panels). Interestingly, Q185R PrP efficiently converted in Ch-N2a58 cells but not in 22L-N2a58 cells (Fig. 3A), where it actually had an inhibitory effect (Fig. 3B, upper panel, and Table 1).

Substitutions of various amino acid species at codons 185 and 218 differentially affect PrP^{Sc} formation between Ch- and 22L-N2a58 cells. To further examine the effect of amino acid substitutions at codons 185 and 218, where strain-specific effects were observed, we replaced each glutamine residue (Q) with various amino acid species, including basic amino acids (R, K, and H), an acidic amino acid (E), and a hydrophobic amino acid (L). As shown in Fig. 4A and Table 1, Q185K, Q185H, and Q185R PrP readily converted to PrP^{Sc} in Ch-N2a58 cells. Interestingly, the amount of Q185K-derived PrP^{Sc} accumulation in Ch-N2a58 cells was higher than that of Mo3F4-derived PrP^{Sc}, suggesting a more efficient conversion of these mutated PrPs in the cells. In contrast, in 22L-N2a58 cells, little PrP^{Sc} derived from Q185R, Q185K, and Q185H PrP accumulated. Q185E and Q185L PrP minimally converted to PrP^{Sc} in both Ch- and 22L-N2a58 cells.

The introduction of substitutions at codon 218, including basic amino acids (R, K, and H), resulted in the loss of conversion in Ch-N2a58 cells (Fig. 4B). Conversely, in 22L-N2a58 cells, Q218R, Q218H, and Q218L efficiently converted to PrP^{Sc}. Q218K PrP did not convert in either cell line (Fig. 4B) and failed to inhibit wild-type Mo3F4 PrP^{Sc} formation (Fig. 2C).

To determine whether different cellular localizations of the mutated PrPs might be the cause of the different conversion effects, we examined the mutated PrPs with indirect immunofluorescence using the 3F4 antibody. Mo3F4, Q185R, Q218R, and Q218K all localized to the cell surface of Ch-N2a58 and 22L-N2a58 cells (data not shown). In addition, phosphatidylinositol-specific phospholipase C treatment removed the mutated PrPs from the cell surface (data not shown). These results demonstrate that the localization of the mutated PrPs cannot account for their strain-specific properties.

Strain-specific properties of the PrP mutations are independent of antibody epitopes. To assess whether the 3F4 epitope can influence the strain-specific properties of the mutated PrPs, we replaced the 3F4 epitope with the L42 epitope (W144Y), because others have previously shown that MoL42 PrP, like Mo3F4 PrP, readily converted to PrP^{Sc} in ScN2a cells (55). Expression of the L42-positive PrPs, MoL42, Q185R, Q218H, Q218R, and Q218K PrPs, was confirmed by Western blotting using the L42 antibody (Fig. 5A, lower panels). The conversion efficiencies of these L42-positive mutated PrPs were similar to those of 3F4-positive mutated PrPs (Fig. 5A, upper panels). Moreover, as shown in Fig. 5B, Q218K PrP again showed strain-dependent effects on MoL42-derived PrP^{Sc}. The data shown in Fig. 5 indicate that changing from a 3F4 epitope to an L42 epitope in the mutant PrPs does not significantly affect their strain-specific effects on PrP^{Sc} formation.

22L and Chandler PrP^{Sc} have different conformations by IR spectra. To assess whether there are any detectable differences in structure between 22L and Chandler PrP^{Sc}, we performed IR spectroscopy. The amide I region (1,600 to 1,700 cm^{-1}) of protein IR spectra is sensitive to differences in protein secondary structure. Although it is difficult to make complete and unequivocal assignments of IR amide I bands, predominantly α-helical and β-sheet proteins have absorption maxima of 1,653 to 1,657 cm^{-1} and 1,615 to 1,640 cm^{-1}, respectively, in water-based (as opposed to D_2O-based) media (see Fig. 7). Unfolded or random-coil polypeptides tend to have absorbance maxima near 1,645 to 1,650 cm^{-1}, and turn structures tend to absorb between 1,660 and 1,680 cm^{-1}. Absorbance maxima are represented by negative deflections in the second-derivative spectra shown in Fig. 7. Previous studies have shown that the infrared spectrum of PrP^{Sc} of different hamster TSE strains can vary markedly despite being composed of PrP molecules of the same amino acid sequence (13, 52). Consistent with that theme, PK-treated PrP^{Sc} isolated from the brains of mice with 22L and Chandler scrapie differed in the IR spectral

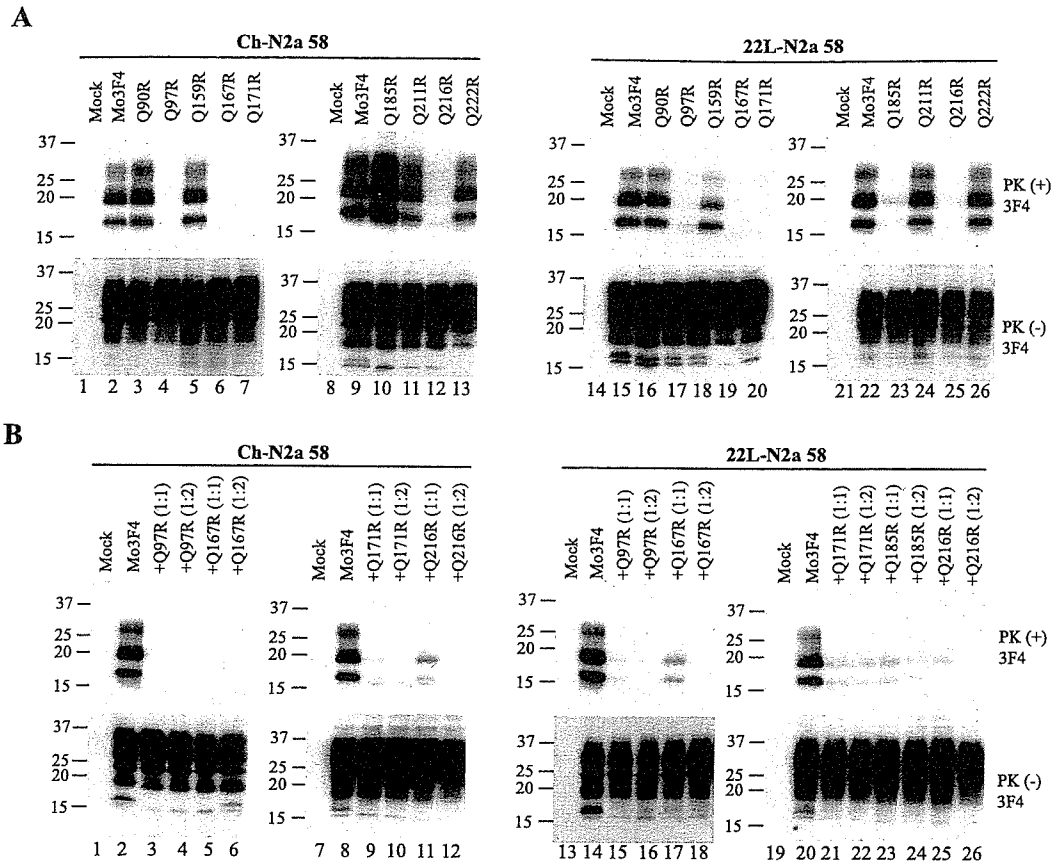

FIG. 3. Strain-specific effects of Q185R mutation on PrP^{Sc} formation. (A) Conversion to 3F4-positive PrP^{Sc} (upper panels) and expression of Mo3F4, Q90R, Q97R, Q159R, Q167R, Q171R, Q185R, Q211R, Q216R, and Q222R (lower panels) were measured by Western blotting using 3F4 antibody. The 3F4 epitope was present in all these constructs. (B) Inhibitory effects of constructs that did not convert were determined by cotransfection with Mo3F4 at a 1:1 or 1:2 DNA ratio. The blots were probed with 3F4 antibody.

region commonly ascribed to the β-sheet region (see Fig. 7). For comparison, PrP^{Sc} from another mouse scrapie strain, 87V, is also shown to have a distinct infrared spectrum in the β-sheet region. In contrast, hemoglobin, a highly α-helical protein, has very little absorbance in the β-sheet region. These results provide direct spectroscopic evidence for differences in conformation between 22L, Chandler, and 87V PrP^{Sc}.

DISCUSSION

In this study, we found evidence that TSE strain characteristics depend on their conformation. We showed that substitutions at codons 185 and 218 resulted in strain-specific PrP^{Sc} formation in cultured neuronal cells infected with two mouse-adapted scrapie prion strains, Chandler and 22L. While others previously demonstrated conformational differences between strains (13, 39, 44, 52), and some strain-specific differences in conformation have been observed in cell-free conversions (6), synthetic amyloid fibrils (25), and purified recombinant *Saccharomyces cerevisiae* Sup35 (31, 49), our results are the first to be obtained from a cell culture comparison of strain effects on the conversion of a panel of mutant PrP^{c} molecules.

The amino acid sequence of PrP can certainly influence the efficiency of transmission of the infectious agent to a new host species (45), but this "species barrier" cannot be explained on the basis of sequence heterogeneity alone. Our results demonstrate that TSE strains with the same sequence have various abilities to convert the PrP^{c} mutants at codons 185 and 218, implying a sequence-independent cause of strain specificity. Although the most efficient conversions are expected to occur between PrP^{c} and PrP^{Sc} with identical sequences, our Q185K mutation promoted PrP^{Sc} formation in Ch-N2a58 cells at a rate higher than that of the homologous wild-type PrP^{c} (Table 1), indicating that sequence homology between PrP^{c} and PrP^{Sc} does not necessarily guarantee the most efficient PrP^{Sc} formation.

The locations of residues 185 and 218 within the secondary structure of PrP may explain why mutations at these sites revealed strain-specific differences in conversion. The nuclear magnetic resonance structure of mouse PrP contains three α-helices comprised of residues 144 to 154, 175 to 193, and 200 to 219; two β-strands containing residues 128 to 131 and 161 to 164; and a disulfide bridge between C178 and C213, linking helices 2 and 3 (42). Amino acid 185 is in helix 2, and residue 218 is in the C-terminal portion of helix 3 (Fig. 6). Helices 2 and 3 and their disulfide bridge are crucial for PrP^{Sc} formation (22, 36), and many point mutations associated with familial human prion diseases are located within or adjacent to these

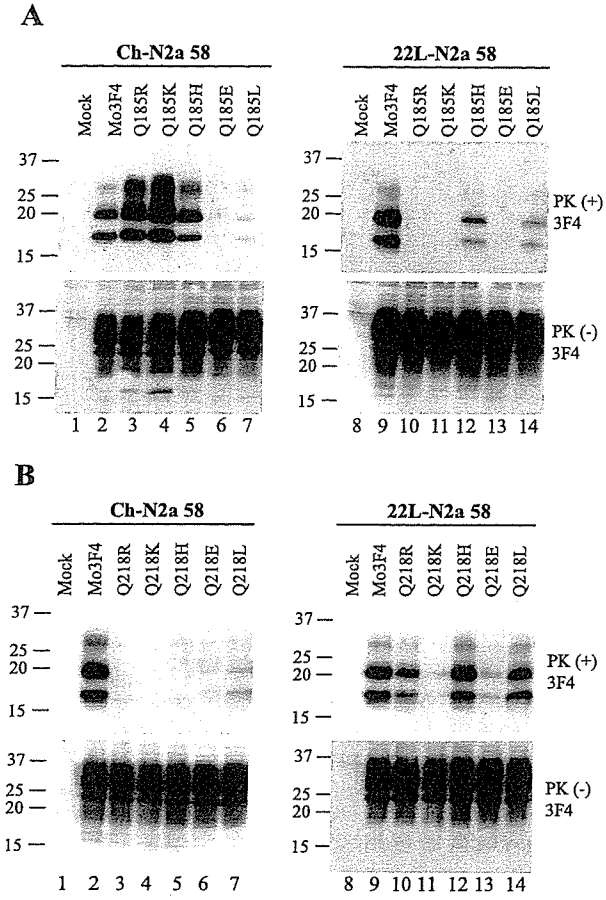

FIG. 4. Strain-specific PrP^{Sc} formation of Q185R, Q185K, Q218R, and Q218H mutated PrP. (A) Conversion to 3F4-positive PrP^{Sc} (upper panels) and expression of Mo3F4, Q185R, Q185K, Q185H, Q185E, and Q185L (lower panels) were measured by Western blot using 3F4 antibody. The 3F4 epitope was present in all these constructs. (B) Western blotting of Mo3F4, Q218R, Q218K, Q218H, Q218E, and Q218L was done as in A.

two helices (41). One such mutation, D178N, is seen in two clinicopathologically distinct diseases, fatal familial insomnia and Creutzfeldt-Jakob disease, the phenotype being determined by the methionine-valine polymorphism at codon 129 of the same mutant allele (21). The striking influence of codon 129 on the D178N mutation phenotype suggests that there may be a modifiable electrostatic interaction or hydrogen bonding between residues 129 and 178 in human PrP (1, 43). Of note, anti-PrP antibody binding studies have revealed that the main conformational differences between PrP^{c} and PrP^{Sc} actually lie toward the N-terminal region in residues 90 to 120, while the C-terminal regions, including helices 2 and 3, remain accessible to antibody in both forms of PrP, implying that their conformation is not significantly altered during conversion (40). This is also consistent with the maintenance of significant α-helical secondary structure content in PrP^{Sc} (13, 14, 38). In addition, a conformation-dependent immunoassay has localized the primary structural differences among PrP^{Sc} strains to their N termini (44). Such observations suggest that helices 2 and 3 may be involved in intra- or intermolecular interactions with the N-terminal domain during PrP^{Sc} formation and may influence the ultimate conformational change of the N terminus, perhaps through an altered β-sheet structure. In keeping with this, our IR spectra detected a difference in β-sheet structures between 22L-PrP^{Sc} and Chandler-PrP^{Sc} (Fig. 7). If these distinct N-terminal domains had differing interactions with helices 2 and 3, particularly around residues 185 and 218, then our mutations may have created structural changes that were compatible with only one of the strains. For example, the introduction of Q185R into helix 2 of mouse PrP^{c} may have interfered with the conformational change of its N-terminal domain into 22L-PrP^{Sc} via steric hindrance and/or electrostatic incompatibility while still allowing its conversion into Chandler-PrP^{Sc}. These strain-specific interactions between the N-terminal domain and helices 2 and 3 are likely quite localized, as mutations at other sites did not reveal any strain differences.

In addition to the location of the mutant residues, the nature of their amino acid change may have contributed to our ob-

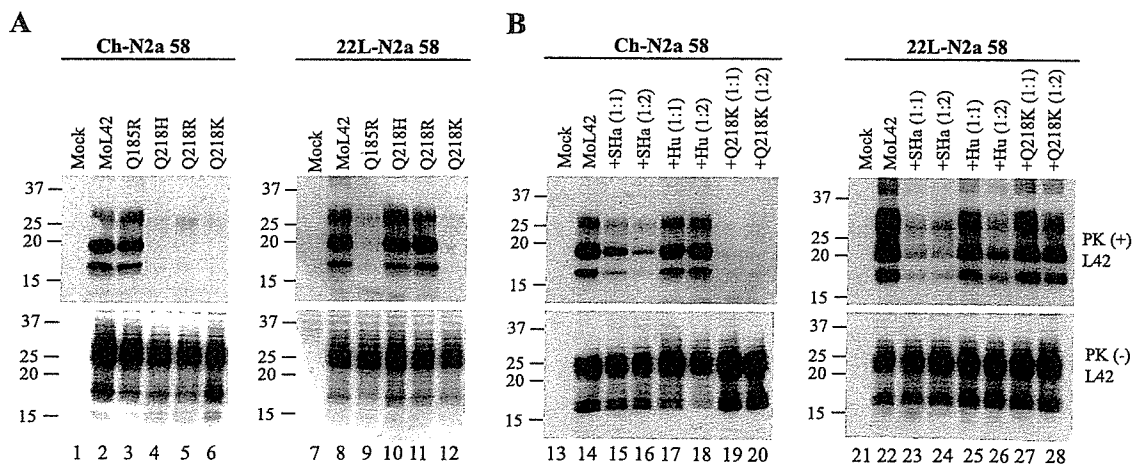

FIG. 5. Strain-specific effects of L42-positive mutated PrPs on PrP^{Sc} formation. (A) Conversion to L42-positive PrP^{Sc} (upper panels) and expression of MoL42, Q185R, Q218H, Q218R, and Q218K (lower panels) were measured by Western blot using L42 antibody. The L42 epitope was present in all these constructs. (B) Inhibitory effects of SHa, Hu, and Q218K were determined by cotransfection with MoL42 at a 1:1 or 1:2 DNA ratio. The blots were probed with the L42 antibody. Molecular mass markers are indicated in kilodaltons on the left side of each panel.

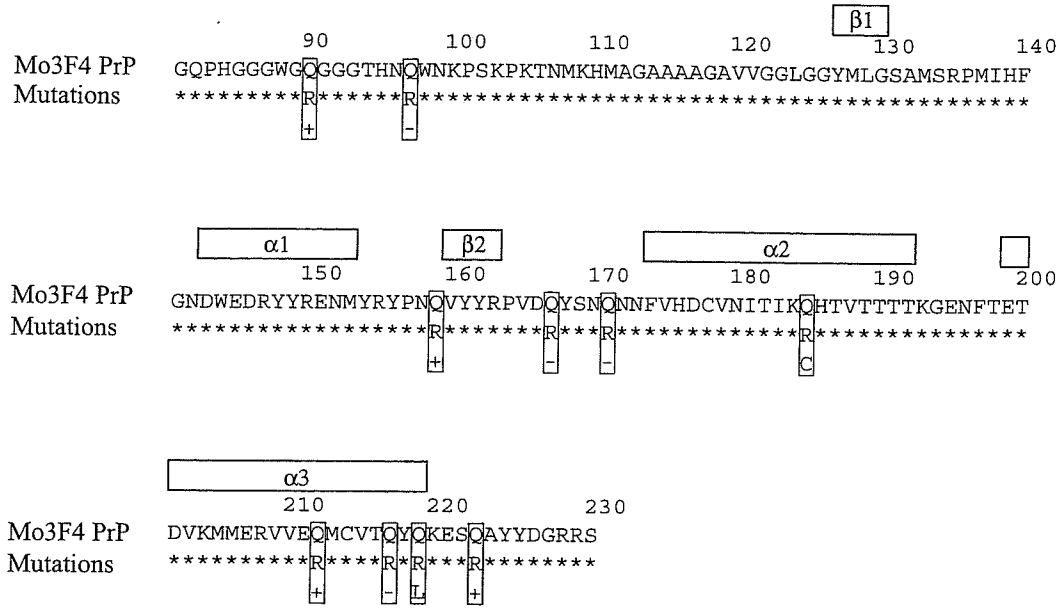

FIG. 6. Amino acid sequence of Mo3F4 and the position of mutations. The amino acid residue number is based on Mo3F4 PrP. The secondary structures in mouse PrP^C are indicated in white boxes at the top. Boxed residues indicate the representative mutations tested; + indicates that conversion occurred in the two cells; − indicates that conversion did not occur in the two cells; "C" indicates Chandler-specific conversion; "L" indicates 22L-specific conversion.

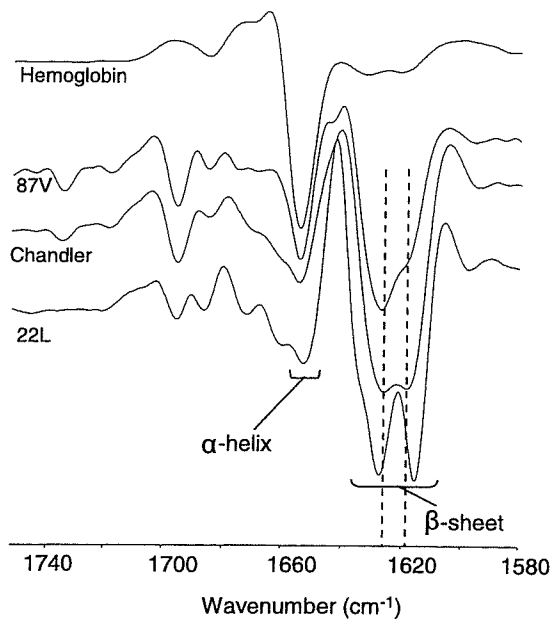

FIG. 7. Comparison of 22L, Chandler, and 87V PrP^{Sc} by infrared spectroscopy. Second-derivative Fourier transform IR spectra are shown for PK-treated PrP^{Sc} samples isolated from the brains of mice affected by either 22L, Chandler, or 87V scrapie. Spectral differences, especially in the β-sheet region of the spectrum, provide evidence that PrP^{Sc} proteins associated with these murine-adapted scrapie strains have distinct conformations. For comparison, a highly α-helical protein, hemoglobin, gives strong absorbance (represented by a negative deflection) at ~1,657 cm^{-1}, with only minor absorbance in the β-sheet region. Similar results were obtained from at least two independent preparations of each strain of PrP^{Sc}.

servations. Similar mutations have been studied to a great extent in yeast, where the translation termination factor Sup35 can aggregate and self-propagate in a prion-like manner. The introduction of point mutations into Sup35 often prevents its aggregation and can block the phenotype of cells that contain aggregated Sup35 (the yeast prion state or [*PSI*]) in a dominant inhibitory fashion. Interestingly, random mutagenesis of Sup35 has revealed that most of these mutants have a glutamine or serine replaced with an arginine (18). Likewise, our PrP mutants, which contained an arginine instead of a glutamine, frequently did not convert and also inhibited the conversion of wild-type PrP. The large, charged arginine side chain most likely has a disruptive effect on the protein-protein interactions that are necessary for aggregation and/or conversion.

Another interesting relationship between our study and those of Sup35 is that in both settings, select mutants have shown strain-specific conversion or aggregation behaviors. When Sup35 aggregates, various levels of translation through premature stop codons can occur, which produces different [*PSI*] phenotypes (53, 58). [*PSI*] strains are heritable and have distinct biological properties that can be propagated in the same yeast genetic background (20). A few Sup35 mutants that displayed different levels of dominant inhibition of [*PSI*], depending on the variant to which they were exposed, have been discovered (19, 30), just as our codon 185 and 218 mutants showed different conversion rates depending on the PrP^{Sc} strain to which they were exposed. The analogous results suggest that various prion types may share similar strain determinants.

A second possibility that could account for the strain-specific properties of our PrP mutations is that the alterations affected interactions between PrP and a strain-specific agent or a host factor. The heterodimer model of the protein-only hypothesis

suggests that an as-yet-unidentified host factor, protein X, is responsible for the behavior of a number of dominant inhibitory forms of PrP^c (26, 51). Interestingly, codon 218 is one of the proposed binding sites for protein X; therefore, a mutation at this site should result in similar conversion rates in cells from the same line, which would have the same protein X. However, in our study, there was a dramatic difference in Q218R and Q218H mutant PrP^{Sc} formation in the same cell line infected with either the Chandler or the 22L strain. Moreover, we and others (55) have shown that PrP mutations with inhibitory effects on conversion are not restricted to the proposed protein X binding sites. There are several previous studies that demonstrated the importance of sulfated glycosaminoglycans (5, 12, 46, 48, 59) and the laminin receptor in PrP^{Sc} formation (33), and more recently, in vitro PrP^{Sc} formation experiments using brain homogenates revealed that host-encoded RNA molecules facilitated PrP^{Sc} formation (17). However, to fully explain how the same mutant PrP^c can convert differently when exposed to two PrP^{Sc} strains, any invoked factor must be associated with the strain itself. For example, the virus or virino hypothesis (15, 27, 34) proposes that agent-encoded nucleic acids are the true determinants of strain diversity. Unfortunately, evidence for such nucleic acids is lacking.

It should be noted that the strain-specific effects were not related to cloning artifacts or the influence of introduced epitopes. Our results were reproduced in other clones and mass cultures prior to cloning (data not shown). In addition, changing the epitope tag from 3F4 to L42 in the mutated PrPs did not affect the strain-specific effects on PrP^{Sc} formation (Fig. 5). This indicated that the properties observed were due only to the codon substitutions.

The best explanation for our data lies with the seeding model hypothesis, which proposes that mutated PrP^c, which is unable to convert, forms a heteropolymer with wild-type PrP^c and PrP^{Sc}, which prevents the conversion of both wild-type and mutated PrP^c. Cell-free conversion studies with purified mouse and hamster PrP isoforms have revealed that heterologous PrP^c, which itself cannot convert, can directly interfere with the conversion of homologous PrP^c into PrP^{Sc}. Furthermore, mouse PrP^c can form heteropolymers with hamster PrP^c and PrP^{Sc} and vice versa (24).

In conclusion, we have shown that mutations at codons 185 and 218 in mouse PrP^c reveal strain-specific effects on PrP^{Sc} formation in cell culture. The conversion differences and IR data suggest that distinct conformations underlie the characteristics of these strains, although the presence of an unidentified strain-specific cofactor cannot be excluded. Further study of these mutants may lead to a better understanding of the structure of PrP^{Sc} and the process by which it is formed. This, in turn, will help advance the knowledge of the molecular basis of TSE strains.

ACKNOWLEDGMENTS

We thank Nobuhiko Okimura for technical assistance, Tsuyoshi Mori for support of indirect immunofluorescence of PrP, and Gregory Raymond for providing brain-derived PrP^{Sc}.

This work was supported by the 21st Century COE Program of Nagasaki University and grants from the Ministry of Education, Culture, Sports, Science, and Technology, Japan, and the Ministry of Health, Labor, and Welfare, Japan. V.L.S. acknowledges support from the Alberta Heritage Foundation for Medical Research through a clinical fellowship award.

REFERENCES

1. **Alonso, D. O., S. J. DeArmond, F. E. Cohen, and V. Daggett.** 2001. Mapping the early steps in the pH-induced conformational conversion of the prion protein. Proc. Natl. Acad. Sci. USA **98**:2985–2989.
2. **Arima, K., N. Nishida, S. Sakaguchi, K. Shigematsu, R. Atarashi, N. Yamaguchi, D. Yoshikawa, J. Yoon, K. Watanabe, N. Kobayashi, S. Mouillet-Richard, S. Lehmann, and S. Katamine.** 2005. Biological and biochemical characteristics of prion strains conserved in persistently infected cell cultures. J. Virol. **79**:7104–7112.
3. **Atarashi, R., N. Nishida, K. Shigematsu, S. Goto, T. Kondo, S. Sakaguchi, and S. Katamine.** 2003. Deletion of N-terminal residues 23–88 from prion protein (PrP) abrogates the potential to rescue PrP-deficient mice from PrP-like protein/Doppel-induced neurodegeneration. J. Biol. Chem. **278**: 28944–28949.
4. **Belt, P. B., I. H. Muileman, B. E. Schreuder, R. Bos-de Ruijter, A. L. Gielkens, and M. A. Smits.** 1995. Identification of five allelic variants of the sheep PrP gene and their association with natural scrapie. J. Gen. Virol. **76**:509–517.
5. **Ben-Zaken, O., S. Tzaban, Y. Tal, L. Horonchik, J. D. Esko, I. Vlodavsky, and A. Taraboulos.** 2003. Cellular heparan sulfate participates in the metabolism of prions. J. Biol. Chem. **278**:40041–40049.
6. **Bessen, R. A., D. A. Kocisko, G. J. Raymond, S. Nandan, P. T. Lansbury, and B. Caughey.** 1995. Non-genetic propagation of strain-specific properties of scrapie prion protein. Nature **375**:698–700.
7. **Bessen, R. A., and R. F. Marsh.** 1992. Biochemical and physical properties of the prion protein from two strains of the transmissible mink encephalopathy agent. J. Virol. **66**:2096–2101.
8. **Birkett, C. R., R. M. Hennion, D. A. Bembridge, M. C. Clarke, A. Chree, M. E. Bruce, and C. J. Bostock.** 2001. Scrapie strains maintain biological phenotypes on propagation in a cell line in culture. EMBO J. **20**:3351–3358.
9. **Bruce, M. E.** 1993. Scrapie strain variation and mutation. Br. Med. Bull. **49**:822–838.
10. **Bruce, M. E.** 2003. TSE strain variation. Br. Med. Bull. **66**:99–108.
11. **Bruce, M. E., I. McConnell, H. Fraser, and A. G. Dickinson.** 1991. The disease characteristics of different strains of scrapie in Sinc congenic mouse lines: implications for the nature of the agent and host control of pathogenesis. J. Gen. Virol. **72**:595–603.
12. **Caughey, B., and G. J. Raymond.** 1993. Sulfated polyanion inhibition of scrapie-associated PrP accumulation in cultured cells. J. Virol. **67**:643–650.
13. **Caughey, B., G. J. Raymond, and R. A. Bessen.** 1998. Strain-dependent differences in beta-sheet conformations of abnormal prion protein. J. Biol. Chem. **273**:32230–32235.
14. **Caughey, B. W., A. Dong, K. S. Bhat, D. Ernst, S. F. Hayes, and W. S. Caughey.** 1991. Secondary structure analysis of the scrapie-associated protein PrP 27–30 in water by infrared spectroscopy. Biochemistry **30**:7672–7680.
15. **Chesebro, B.** 2003. Introduction to the transmissible spongiform encephalopathies or prion diseases. Br. Med. Bull. **66**:1–20.
16. **Collinge, J., K. C. Sidle, J. Meads, J. Ironside, and A. F. Hill.** 1996. Molecular analysis of prion strain variation and the aetiology of 'new variant' CJD. Nature **383**:685–690.
17. **Deleault, N. R., R. W. Lucassen, and S. Supattapone.** 2003. RNA molecules stimulate prion protein conversion. Nature **425**:717–720.
18. **DePace, A. H., A. Santoso, P. Hillner, and J. S. Weissman.** 1998. A critical role for amino-terminal glutamine/asparagine repeats in the formation and propagation of a yeast prion. Cell **93**:1241–1252.
19. **Derkatch, I. L., M. E. Bradley, P. Zhou, and S. W. Liebman.** 1999. The PNM2 mutation in the prion protein domain of SUP35 has distinct effects on different variants of the [PSI+] prion in yeast. Curr. Genet. **35**:59–67.
20. **Derkatch, I. L., Y. O. Chernoff, V. V. Kushnirov, S. G. Inge-Vechtomov, and S. W. Liebman.** 1996. Genesis and variability of [PSI] prion factors in Saccharomyces cerevisiae. Genetics **144**:1375–1386.
21. **Goldfarb, L. G., R. B. Petersen, M. Tabaton, P. Brown, A. C. LeBlanc, P. Montagna, P. Cortelli, J. Julien, C. Vital, W. W. Pendelbury, M. Haltia, P. R. Wills, J. J. Hauw, P. E. McKeever, L. Monari, B. Schrank, G. D. Swergold, L. Autilio-Gambetti, D. C. Gajdusek, E. Lugaresi, and P. Gambetti.** 1992. Fatal familial insomnia and familial Creutzfeldt-Jakob disease: disease phenotype determined by a DNA polymorphism. Science **258**:806–808.
22. **Herrmann, L. M., and B. Caughey.** 1998. The importance of the disulfide bond in prion protein conversion. Neuroreport **9**:2457–2461.
23. **Hill, A. F., M. Desbruslais, S. Joiner, K. C. Sidle, I. Gowland, J. Collinge, L. J. Doey, and P. Lantos.** 1997. The same prion strain causes vCJD and BSE. Nature **389**:448–450, 526.
24. **Horiuchi, M., S. A. Priola, J. Chabry, and B. Caughey.** 2000. Interactions between heterologous forms of prion protein: binding, inhibition of conversion, and species barriers. Proc. Natl. Acad. Sci. USA **97**:5836–5841.
25. **Jones, E. M., and W. K. Surewicz.** 2005. Fibril conformation as the basis of species- and strain-dependent seeding specificity of mammalian prion amyloids. Cell **121**:63–72.

26. **Kaneko, K., L. Zulianello, M. Scott, C. M. Cooper, A. C. Wallace, T. L. James, F. E. Cohen, and S. B. Prusiner.** 1997. Evidence for protein X binding to a discontinuous epitope on the cellular prion protein during scrapie prion propagation. Proc. Natl. Acad. Sci. USA **94**:10069–10074.
27. **Kimberlin, R. H.** 1982. Scrapie agent: prions or virions? Nature **297**:107–108.
28. **Kimberlin, R. H., S. Cole, and C. A. Walker.** 1987. Temporary and permanent modifications to a single strain of mouse scrapie on transmission to rats and hamsters. J. Gen. Virol. **68**:1875–1881.
29. **Kimberlin, R. H., C. A. Walker, and H. Fraser.** 1989. The genomic identity of different strains of mouse scrapie is expressed in hamsters and preserved on reisolation in mice. J. Gen. Virol. **70**:2017–2025.
30. **King, C. Y.** 2001. Supporting the structural basis of prion strains: induction and identification of [PSI] variants. J. Mol. Biol. **307**:1247–1260.
31. **King, C. Y., and R. Diaz-Avalos.** 2004. Protein-only transmission of three yeast prion strains. Nature **428**:319–323.
32. **Korth, C., K. Kaneko, D. Groth, N. Heye, G. Telling, J. Mastrianni, P. Parchi, P. Gambetti, R. Will, J. Ironside, C. Heinrich, P. Tremblay, S. J. DeArmond, and S. B. Prusiner.** 2003. Abbreviated incubation times for human prions in mice expressing a chimeric mouse-human prion protein transgene. Proc. Natl. Acad. Sci. USA **100**:4784–4789.
33. **Leucht, C., S. Simoneau, C. Rey, K. Vana, R. Rieger, C. I. Lasmezas, and S. Weiss.** 2003. The 37 kDa/67 kDa laminin receptor is required for PrP(Sc) propagation in scrapie-infected neuronal cells. EMBO Rep. **4**:290–295.
34. **Manuelidis, L.** 2003. Transmissible encephalopathies: speculations and realities. Viral Immunol. **16**:123–139.
35. **Meyer, R. K., M. P. McKinley, K. A. Bowman, M. B. Braunfeld, R. A. Barry, and S. B. Prusiner.** 1986. Separation and properties of cellular and scrapie prion proteins. Proc. Natl. Acad. Sci. USA **83**:2310–2314.
36. **Muramoto, T., M. Scott, F. E. Cohen, and S. B. Prusiner.** 1996. Recombinant scrapie-like prion protein of 106 amino acids is soluble. Proc. Natl. Acad. Sci. USA **93**:15457–15462.
37. **Nishida, N., D. A. Harris, D. Vilette, H. Laude, Y. Frobert, J. Grassi, D. Casanova, O. Milhavet, and S. Lehmann.** 2000. Successful transmission of three mouse-adapted scrapie strains to murine neuroblastoma cell lines overexpressing wild-type mouse prion protein. J. Virol. **74**:320–325.
38. **Pan, K. M., M. Baldwin, J. Nguyen, M. Gasset, A. Serban, D. Groth, I. Mehlhorn, Z. Huang, R. J. Fletterick, F. E. Cohen, and S. B. Prusiner.** 1993. Conversion of alpha-helices into beta-sheets features in the formation of the scrapie prion proteins. Proc. Natl. Acad. Sci. USA **90**:10962–10966.
39. **Peretz, D., M. R. Scott, D. Groth, R. A. Williamson, D. R. Burton, F. E. Cohen, and S. B. Prusiner.** 2001. Strain-specified relative conformational stability of the scrapie prion protein. Protein Sci. **10**:854–863.
40. **Peretz, D., R. A. Williamson, Y. Matsunaga, H. Serban, C. Pinilla, R. B. Bastidas, R. Rozenshteyn, T. L. James, R. A. Houghten, F. E. Cohen, S. B. Prusiner, and D. R. Burton.** 1997. A conformational transition at the N terminus of the prion protein features in formation of the scrapie isoform. J. Mol. Biol. **273**:614–622.
41. **Prusiner, S. B., M. R. Scott, S. J. DeArmond, and F. E. Cohen.** 1998. Prion protein biology. Cell **93**:337–348.
42. **Riek, R., S. Hornemann, G. Wider, M. Billeter, R. Glockshuber, and K. Wuthrich.** 1996. NMR structure of the mouse prion protein domain PrP(121–321). Nature **382**:180–182.
43. **Riek, R., G. Wider, M. Billeter, S. Hornemann, R. Glockshuber, and K. Wuthrich.** 1998. Prion protein NMR structure and familial human spongiform encephalopathies. Proc. Natl. Acad. Sci. USA **95**:11667–11672.
44. **Safar, J., H. Wille, V. Itri, D. Groth, H. Serban, M. Torchia, F. E. Cohen, and S. B. Prusiner.** 1998. Eight prion strains have PrP(Sc) molecules with different conformations. Nat. Med. **4**:1157–1165.
45. **Scott, M., D. Foster, C. Mirenda, D. Serban, F. Coufal, M. Walchli, M. Torchia, D. Groth, G. Carlson, S. J. DeArmond, D. Westaway, and S. B. Prusiner.** 1989. Transgenic mice expressing hamster prion protein produce species-specific scrapie infectivity and amyloid plaques. Cell **59**:847–857.
46. **Shaked, G. M., Z. Meiner, I. Avraham, A. Taraboulos, and R. Gabizon.** 2001. Reconstitution of prion infectivity from solubilized protease-resistant PrP and nonprotein components of prion rods. J. Biol. Chem. **276**:14324–14328.
47. **Shibuya, S., J. Higuchi, R. W. Shin, J. Tateishi, and T. Kitamoto.** 1998. Codon 219 Lys allele of PRNP is not found in sporadic Creutzfeldt-Jakob disease. Ann. Neurol. **43**:826–828.
48. **Snow, A. D., R. Kisilevsky, J. Willmer, S. B. Prusiner, and S. J. DeArmond.** 1989. Sulfated glycosaminoglycans in amyloid plaques of prion diseases. Acta Neuropathol. (Berlin) **77**:337–342.
49. **Tanaka, M., P. Chien, N. Naber, R. Cooke, and J. S. Weissman.** 2004. Conformational variations in an infectious protein determine prion strain differences. Nature **428**:323–328.
50. **Telling, G. C., P. Parchi, S. J. DeArmond, P. Cortelli, P. Montagna, R. Gabizon, J. Mastrianni, E. Lugaresi, P. Gambetti, and S. B. Prusiner.** 1996. Evidence for the conformation of the pathologic isoform of the prion protein enciphering and propagating prion diversity. Science **274**:2079–2082.
51. **Telling, G. C., M. Scott, J. Mastrianni, R. Gabizon, M. Torchia, F. E. Cohen, S. J. DeArmond, and S. B. Prusiner.** 1995. Prion propagation in mice expressing human and chimeric PrP transgenes implicates the interaction of cellular PrP with another protein. Cell **83**:79–90.
52. **Thomzig, A., S. Spassov, M. Friedrich, D. Naumann, and M. Beekes.** 2004. Discriminating scrapie and bovine spongiform encephalopathy isolates by infrared spectroscopy of pathological prion protein. J. Biol. Chem. **279**: 33847–33854.
53. **Uptain, S. M., and S. Lindquist.** 2002. Prions as protein-based genetic elements. Annu. Rev. Microbiol. **56**:703–741.
54. **Vorberg, I., A. Buschmann, S. Harmeyer, A. Saalmuller, E. Pfaff, and M. H. Groschup.** 1999. A novel epitope for the specific detection of exogenous prion proteins in transgenic mice and transfected murine cell lines. Virology **255**:26–31.
55. **Vorberg, I., M. H. Groschup, E. Pfaff, and S. A. Priola.** 2003. Multiple amino acid residues within the rabbit prion protein inhibit formation of its abnormal isoform. J. Virol. **77**:2003–2009.
56. **Weissmann, C.** 2004. The state of the prion. Nat. Rev. Microbiol. **2**:861–871.
57. **Westaway, D., V. Zuliani, C. M. Cooper, M. Da Costa, S. Neuman, A. L. Jenny, L. Detwiler, and S. B. Prusiner.** 1994. Homozygosity for prion protein alleles encoding glutamine-171 renders sheep susceptible to natural scrapie. Genes Dev. **8**:959–969.
58. **Wickner, R. B., H. K. Edskes, B. T. Roberts, U. Baxa, M. M. Pierce, E. D. Ross, and A. Brachmann.** 2004. Prions: proteins as genes and infectious entities. Genes Dev. **18**:470–485.
59. **Wong, C., L. W. Xiong, M. Horiuchi, L. Raymond, K. Wehrly, B. Chesebro, and B. Caughey.** 2001. Sulfated glycans and elevated temperature stimulate PrP(Sc)-dependent cell-free formation of protease-resistant prion protein. EMBO J. **20**:377–386.

Available online at www.sciencedirect.com
ScienceDirect
Gene 386 (2007) 139–146
GENE
SECTION
FUNCTIONAL GENOMICS
www.elsevier.com/locate/gene

Newly established *in vitro* system with fluorescent proteins shows that abnormal expression of downstream prion protein-like protein in mice is probably due to functional disconnection between splicing and 3′ formation of prion protein pre-mRNA

Daisuke Yoshikawa [a], Juraj Kopacek [a,b], Naohiro Yamaguchi [a], Daisuke Ishibashi [c], Hitoki Yamanaka [c], Yoshitaka Yamaguchi [c], Shigeru Katamine [a], Suehiro Sakaguchi [a,c,d,*]

[a] *Department of Molecular Microbiology and Immunology, Nagasaki University Graduate School of Biomedical Sciences, Sakamoto 1-12-4, Nagasaki 852-8523, Japan*
[b] *Department of Molecular Biology, Institute of Virology, Slovak Academy of Sciences, Bratislava, Slovakia*
[c] *PRESTO Japan Science and Technology Agency, 4-1-8 Honcho Kawaguchi, Saitama, Japan*
[d] *Division of Molecular Cytology, Institute for Enzyme Research, The University of Tokushima, 3-18-15 Kuramoto-cho, Tokushima 770-8503, Japan*

Received 10 July 2006; received in revised form 8 August 2006; accepted 25 August 2006
Available online 15 September 2006
Received by A. Bernardi

Abstract

We and others previously showed that, in some lines of prion protein (PrP)-knockout mice, the downstream PrP-like protein (PrPLP/Dpl) was abnormally expressed in brains partly due to impaired cleavage/polyadenylation of the residual PrP promoter-driven pre-mRNA despite the presence of a poly(A) signal. In this study, we newly established an *in vitro* transient transfection system in which abnormal expression of PrPLP/Dpl can be visualized by expression of the green fluorescence protein, EGFP, in cultured cells. No EGFP was detected in cells transfected by a vector carrying a PrP genomic fragment including the region targeted in the knockout mice intact upstream of the PrPLP/Dpl gene. In contrast, deletion of the targeted region from the vector caused expression of EGFP. By employing this system with other vectors carrying various deletions or point mutations in the targeted region, we identified that disruption of the splicing elements in the PrP terminal intron caused the expression of EGFP. Recent lines of evidence indicate that terminal intron splicing and cleavage/polyadenylation of pre-mRNA are functionally linked to each other. Taken together, our newly established system shows that the abnormal expression of PrPLP/Dpl in PrP-knockout mice caused by the impaired cleavage/polyadenylation of the PrP promoter-driven pre-mRNA is due to the functional dissociation between the pre-mRNA machineries, in particular those of cleavage/polyadenylation and splicing. Our newly established *in vitro* system, in which the functional dissociation between the pre-mRNA machineries can be visualized by EGFP green fluorescence, may be useful for studies of the functional connection of pre-mRNA machineries.

Keywords: Intergenic splicing; *In vitro* system; Purkinje cell degeneration; Fluorescent protein

1. Introduction

Prnd is a recently identified gene encoding the first prion protein (PrP)-like protein, PrPLP/Doppel (Dpl), locating 16-kb downstream of the PrP gene, *Prnp* (Moore et al., 1999; Li et al., 2000a). *Prnd* is actively expressed in the testis, heart, skeletal muscle, and spleen, but not in the brain, whereas *Prnp* is the most abundantly expressed in the brain (Li et al., 2000b). Male mice devoid of PrPLP/Dpl were shown to be infertile due to

Abbreviations: PrP, prion protein; PrPLP/Dpl, PrP-like protein/Doppel; bp, base pair; PCR, polymerase chain reaction; nt, nucleotides; EGFP, enhanced green fluorescence protein; UTR, untranslated region; ORF, open reading frame; DMEM, Dulbecco's Modified Eagle Medium; RACE, rapid amplification of cDNA ends; HCMV, human cytomegalovirus; RNP, ribonucleoprotein; PAP, poly(A) polymerase; CPSF, cleavage/polyadenylation specificity factor.

* Corresponding author. Division of Molecular Cytology, Institute for Enzyme Research, The University of Tokushima, 3-18-15 Kuramoto-cho, Tokushima 770-8503, Japan. Tel.: +81 88 633 7438; fax: +81 88 633 7440.
E-mail address: sakaguch@ier.tokushima-u.ac.jp (S. Sakaguchi).

0378-1119/$ - see front matter © 2006 Elsevier B.V. All rights reserved.
doi:10.1016/j.gene.2006.08.028

abnormal development of sperm, indicating that PrPLP/Dpl is important for spermatogenesis (Behrens et al., 2002).

We and others found that PrPLP/Dpl is toxic when ectopically expressed in neurons deficient for the cellular PrP (PrP^C) (Moore et al., 2001; Anderson et al., 2004; Yamaguchi et al., 2004). Some lines of mice devoid of PrP^C (*Prnp*$^{0/0}$), including Ngsk *Prnp*$^{0/0}$, Rcm0 *Prnp*$^{0/0}$, and Zrch II *Prnp*$^{0/0}$, developed ataxia and Purkinje cell degeneration due to the ectopic expression of PrPLP/Dpl in neurons, but others, such as Zrch I *Prnp*$^{0/0}$ and Npu *Prnp*$^{0/0}$, showed neither the ectopic expression of PrPLP/Dpl nor such neurological abnormalities (Bueler et al., 1992; Manson et al., 1994; Sakaguchi et al., 1996; Moore et al., 1999; Rossi et al., 2001). In the ataxic lines of *Prnp*$^{0/0}$ mice, *Prnd* was aberrantly regulated under the control of *Prnp* promoter and thereby ectopically expressed in the brain, especially in neurons, where the *Prnp* promoter is very active (Moore et al., 1999; Li et al., 2000a). The ectopically expressing PrPLP/Dpl mRNAs were chimeric, comprising the residual *Prnp* non-coding exons 1 and 2 at the 5′ end followed by the *Prnd*-coding exons, due to an abnormal intergenic splicing taking place between *Prnp* and *Prnd* (Moore et al., 1999; Li et al., 2000a). The mechanism of how *Prnd* became abnormally regulated under the control of the *Prnp* promoter in the ataxic lines of *Prnp*$^{0/0}$ mice remains to be studied.

In wild-type mice, PrP pre-mRNA is normally cleaved and polyadenylated at the end of *Prnp*. However, in ataxic lines of *Prnp*$^{0/0}$ mice, the pre-mRNA was unsuccessfully cleaved and polyadenylated at the end of *Prnp*, resulting in its elongation until the end of downstream *Prnd* (Moore et al., 1999; Li et al., 2000a), indicating that the abnormal regulation of *Prnd* in these mice could be in part attributable to the impaired cleavage/polyadenylation of *Prnp* pre-mRNA. A polyadenylation signal is essential for the pre-mRNA cleavage/polyadenylation processes. However, the polyadenylation signal of *Prnp* and its flanking sequences are intact in two ataxic lines of Ngsk *Prnp*$^{0/0}$ and Rcm0 *Prnp*$^{0/0}$ mice. It is recently believed that the pre-mRNA processes, including acquisition of a cap structure at the 5′ end, splicing out of introns, and cleavage/polyadenylation at the 3′ end, are functionally linked to each other during transcription (Steinmetz, 1997; Proudfoot et al., 2002; Kornblihtt et al., 2004). In particular, the cleavage/polyadenylation processes are strongly influenced by splicing of the terminal intron. In the ataxic lines of *Prnp*$^{0/0}$ mice, a part of the *Prnp* terminal intron including the elements important for splicing, such as a splice branch point, a polypyrimidine tract, and a splice acceptor, is commonly targeted as well as the subsequent half of the last exon (Sakaguchi et al., 1995; Moore et al., 1999; Rossi et al., 2001). Thus, disruption of these splicing elements due to deletion of intron 2 could cause functional dissociation between splicing and cleavage/polyadenylation for the *Prnp* pre-mRNA in the ataxic lines of *Prnp*$^{0/0}$ mice, resulting in the impaired cleavage/polyadenylation of the pre-mRNA. It is alternatively possible that deletion of the exonic sequences in *Prnp* might disturb the cleavage/polyadenylation processes for the *Prnp* pre-mRNA.

In the present study, we established an *in vitro* transient transfection system in which abnormal expression of PrPLP/Dpl can be visualized by expression of the green fluorescence protein, EGFP, in cultured cells. Using this system, we identified that the abnormal expression of PrPLP/Dpl could be attributed to the functional disconnection between splicing and cleavage/polyadenylation processes. These results indicate usefulness of our newly established *in vitro* system for studying the functional connection of pre-mRNA machineries because the functional dissociation between the pre-mRNA machineries can be easily visualized by EGFP green fluorescence.

2. Materials and methods

2.1. Expression vectors

2.1.1. pPrPwild

The 488- and 2688-bp genomic fragments of *Prnd*, spanning nucleotides (nt) 35,716 to 36,204 (GenBank accession no. *U29187*) and nt 36,712 to 39,400, respectively, were first amplified from mouse genomic DNA using polymerase chain reaction (PCR; Advantage cDNA PCR KIT, Clontech, California, USA) with appropriate sets of a primer pair. The former, corresponding to a part of intron 1 and an entire 5′ untranslated region (UTR) of *Prnd*, possessed the *Sal* I and *Nhe* I enzyme sites at the 5′ and 3′ ends, respectively. The latter, consisting of an entire 3′ UTR and the downstream intervening sequence, had the *Bam*H I and *Mlu* I sites at its 5′ and 3′ ends, respectively. These fragments were ligated with the enhanced green fluorescence protein (EGFP)-coding *Nhe* I–*Bam*H I insert of pEGFP-C1 (Clontech) in such a way that the EGFP insert was flanked by the genomic fragments, and cloned into the *Sal* I and *Mlu* I sites of a pDON-AI plasmid (Takara, Tokyo, Japan) with a newly created *Mlu* I site at the multiple cloning site, yielding the plasmid pPrnd-EGFP. Next, two *Prnp* genomic DNAs, the 806-bp fragment from nt 18,861 to 19,667 encompassing a part of intron 2 and an entire 5′ UTR of exon 3 and the 1699-bp DNA from nt 20,442 to 22,140 consisting of an entire 3′ UTR and the downstream intervening sequence, were amplified by PCR. The former possessed the artificial *Spe* I and *Bam*H I enzyme sites at the 5′ and 3′ ends, respectively, and the latter contained the *Not* I and *Sal* I sites at the 5′ and 3′ ends, respectively. These fragments were ligated with the DsRed-coding *Bam*H I–*Not* I insert of pDsRed1-N1 (Clontech) in such a way that the insert was flanked by the two genomic fragments, and cloned into the *Spe* I and *Sal* I sites of pPrnd-EGFP, resulting in pPrPwild.

2.1.2. pPrP5′targeted

The 750-bp (from nt 18,661 to 19,411) fragment of *Prnp* intron 2, containing *Spe* I and *BamH* I sites at the 5′ and 3′ ends, respectively, was generated by PCR with a primer pair, and then placed for the corresponding fragment in pPrPwild, resulting in pPrP5′targeted.

2.1.3. pPrPint2(-3), pPrPint2(-26), pPrPint2(-50)

The *Prnp* intron 2 containing either 3-bp from nt 19,664 to 19,666, 26-bp from nt 19,641 to 19,666, or 50-bp from nt 19,617 to 19,666, together with the 5′ UTR of exon 3 and the

DsRed open reading frame (ORF), was amplified by PCR with a primer pair using pPrPwild as a template. *Bgl* II and *Not* I sites were introduced at the 5′ and 3′ ends of each fragment, respectively. These amplified fragments were placed for the corresponding fragment in pPrP5′targeted, respectively, yielding pPrPint2(-3), pPrPint2(-26) and pPrPint2(-50).

2.1.4. pPrP3′targeted and pPrPtargeted

A genomic fragment from nt 20,893 (corresponding to the *Eco*R I site in *Prnp* exon 3) to 22,140, encompassing a part of 3′ UTR and the downstream intervening sequence, was amplified by PCR using pPrPwild as a template with primers, each containing the *Not* I or *Sal* I recognition sequences. This amplified fragment was placed for the corresponding *Not* I–*Sal* I fragment in pPrPwild, producing a pPrP3′targeted plasmid. Moreover, pPrPtargeted was constructed by replacing this amplified fragment with the corresponding fragment in pPrP5′ targeted.

2.1.5. pPrPint2(-26)AG, pPrPint2(-26)Br, pPrPint2(-26)Br2×, pPrPint2(-26)AGBr2×

To construct these vectors, point mutations were introduced using a QuickChange Site-Directed Mutagenesis Kit (Stratagen, La Jolla, CA) using pPrPint2(-26) as a template. The mutations were verified by DNA sequencing.

2.2. Transfection and fluorescent microscopic analysis

Plasmids were transfected into mouse neuroblastoma N2a cells, which were maintained at 37 °C under 5% CO_2 in Dulbecco's Modified Eagle Medium (DMEM) supplemented with 10% fetal bovine serum. 2×10^5 cells were plated in one well of a 6-well plate and transfected by plasmids using Lipofectamin 2000 reagent (Invitrogen life technologies, Carlsbad, CA) the next day, as recommended by the manufacturer. Cells were inspected 48 h after transfection by fluorescence microscopy.

2.3. 3′ Rapid amplification of cDNA ends (RACE)

Total RNA was isolated from the cells 48 h after transfection using a Trizol reagent (Invitrogen life technologies). 1 μg of total RNA was subjected to first strand cDNA synthesis with Oligo dT-3 sites Adaptor Primer using the 3′-Full RACE Core Set (Takara) according to the manufacturer's recommendations. The synthesized cDNAs were subsequently amplified directly by PCR using the R-U5-3* primer, 5′-AGTGATTGACTACCC GTCAGCGGGGGTC-3′, and the 3 sites Adaptor Primer, 5′-CTGATCTAGAGGTACCGGATCC-3′.

2.4. DNA sequencing

DNA sequences were determined by the chain termination reaction method using Texas Red labeled specific primers (Amersham) and the ThermoSequenase premixed cycle sequencing kit (Amersham) according to the manufacturer's recommendations.

3. Results and discussion

3.1. Establishment of an in vitro transient transfection system to easily detect abnormal expression of PrPLP/Dpl by EGFP fluorescent protein

To establish an *in vitro* transient transfection system, in which the intergenic splicing-mediated abnormal expression of PrPLP/Dpl in ataxic lines of $Prnp^{0/0}$ mice can be mimicked in cultured cells, we first constructed two expression vectors, termed pPrPwild and pPrPtargeted. pPrPwild contained a part of *Prnp* genomic DNA including 816-bp of the 3′ part of intron 2, the entire exon 3, and the 3′ intervening sequence, followed by a *Prnd* genomic fragment comprising intron 1, exon 2, intron 2, exon 3 and the 3′ intervening sequence (Fig. 1B). In this vector, transcription is engineered to start from the upstream vector-derived exon under the control of the immediate early gene promoter of human cytomegalovirus (HCMV) and terminate at the end of *Prnp* exon 3 using its native poly(A) signal (Fig. 1B). We also replaced the *Prnp*- and *Prnd*-coding sequences with those of the fluorescent proteins, DsRed and EGFP, respectively (Fig. 1B), to easily detect expression of the *Prnp*- or the *Prnd*-coding exon under fluorescence microscopy. pPrPtargeted lacks the same *Prnp* region as in the ataxic lines of $Prnp^{0/0}$ mice, including 250-bp of intron 2, 10-bp of the 5′ UTR, the entire PrP ORF, and 450-bp of the 3′ UTR (Fig. 1A and B).

We then transfected these vectors into mouse N2a neuroblastoma cells and carried out a fluorescent microscopic examination 48 h after transfection. We also characterized the transcripts expressed from the vectors in these transfected cells by a 3′ RACE cloning technique and subsequent DNA sequencing. The pPrPwild-transfected cells produced DsRed fluorescence alone (Fig. 1C). No EGFP expression could be detected in these cells (Fig. 1C). 3′ RACE of the total RNA extracted from these transfected cells revealed several distinct bands, including one major and a few minor bands, on an agarose gel (Fig. 2A). We cloned the major band and determined its DNA sequence. The major transcript consisted of the vector-derived exon and *Prnp* exon 3 followed by a poly(A) tail (Fig. 2B), indicating that transcription was started from the vector-derived exon, terminating at the end of the *Prnp* exon 3, being subjected to splicing between these two exons. In contrast, pPrPtargeted produced only green EGFP but not DsRed fluorescence in the cells (Fig. 1C). 3′ RACE of these cells produced one major and a few minor bands on an agarose gel (Fig. 2A). DNA sequencing of the major band showed that it comprised the vector-derived exon and the downstream *Prnd* exons (Fig. 2B), indicating that the pre-mRNA started from the vector-derived exon was unsuccessfully terminated at the end of the *Prnp* terminal exon 3, elongated to the *Prnd* terminal exon 3, and subsequently underwent aberrant splicing between the vector-derived exon and the *Prnd* exons 2 and 3. This abnormal processing of the pre-mRNA expressed from pPrPtargeted in N2a cells is very similar to that for the targeted *Prnp* allele in the ataxic lines of $Prnp^{0/0}$ mice (Moore et al., 1999; Li et al., 2000a), whereas the processing for the pre-mRNA in the cells transfected

by pPrPwild is similar to that in wild-type mice. These results indicate that our newly established *in vitro* transient transfection system could reproduce the abnormal expression of PrPLP/Dpl in the ataxic lines of $Prnp^{0/0}$ mice in cultured cells by expression of EGFP fluorescent protein. Since pPrPtargeted lacks the *Prnp* sequences commonly targeted in the ataxic lines of $Prnp^{0/0}$ mice (Sakaguchi et al., 1995; Moore et al., 1999; Rossi et al., 2001), it is conceivable that the abnormal expression of PrPLP/Dpl in the ataxic lines of $Prnp^{0/0}$ mice is very likely due to deletion of a *cis*-element(s) present in the commonly targeted *Prnp* sequences.

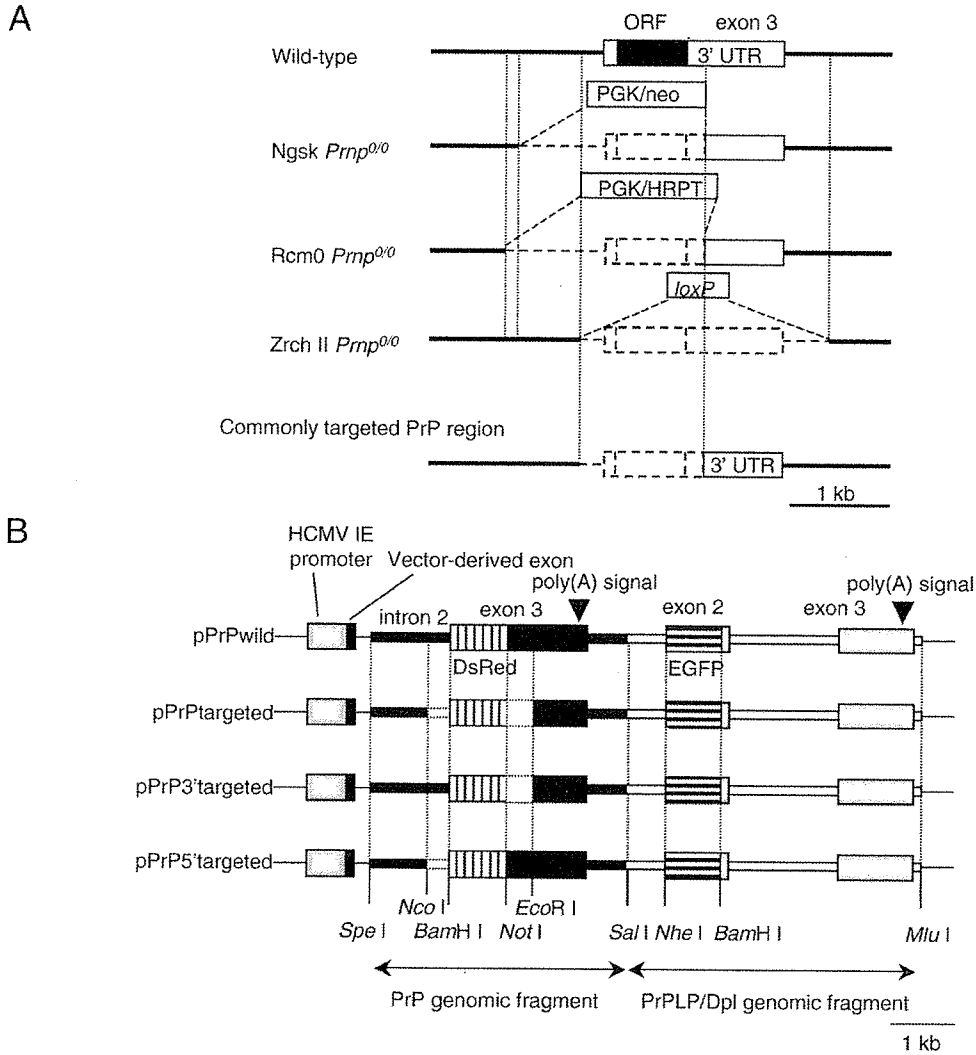

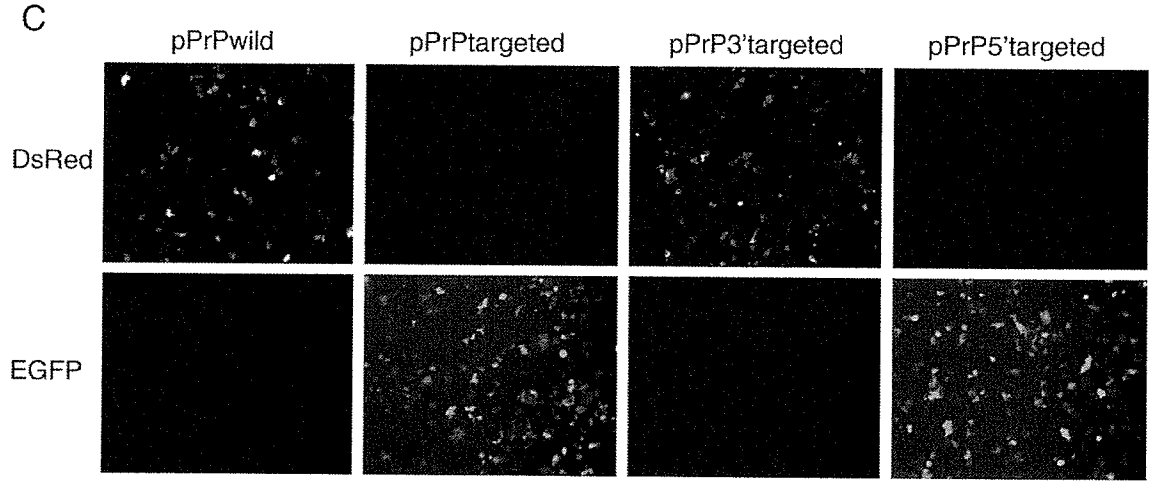

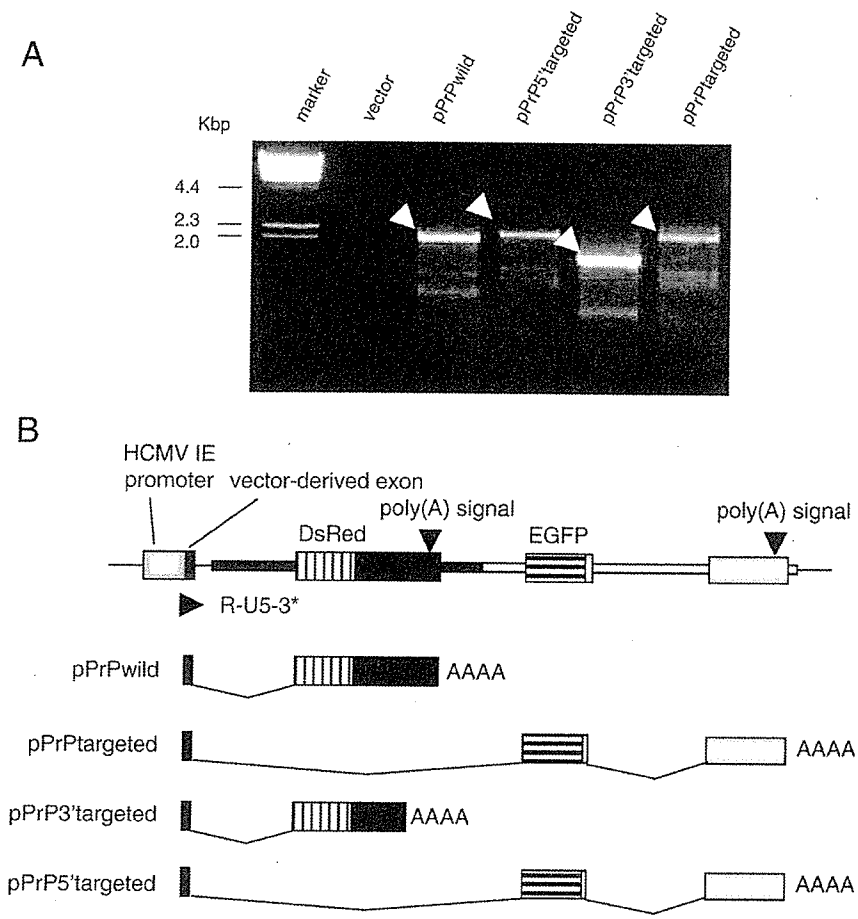

Fig. 2. (A) 3′ RACE of N2a cells 48 h after transient transfection of pPrPwild, pPrPtargeted, pPrP3′targeted, and pPrP5′targeted. Several distinct bands including one major band (indicated by arrow heads) are visible in each lane. (B) Schematic structures of the major transcripts expressed in the transfected N2a cells. These structures were determined on the basis of the DNA sequence of each major band. All poly(A) signals are native. AAAA indicates a poly(A) tail. R-U5-3* is a primer used for 3′ RACE.

3.2. Abnormal expression of PrPLP/Dpl assessed in the in vitro transient transfection system with vectors carrying various deletions in the upstream Prnp sequence

To employ our newly established *in vitro* system to investigate the genetic mechanism of the abnormal expression of PrPLP/Dpl in the ataxic lines of $Prnp^{0/0}$ mice, we constructed two other vectors, pPrP3′targeted and pPrP5′targeted. pPrP3′targeted lacks 450-bp of the *Prnp* 3′ UTR whereas pPrP5′targeted lacks 249-bp of intron 2 and 10-bp of the 5′ UTR (Fig. 1B). We transfected pPrP3′targeted and pPrP5′targeted into N2a cells. pPrP3′targeted expressed DsRed but not EGFP fluorescence in N2a cells 48 h after transfection (Fig. 1C). 3′ RACE and DNA sequencing showed that the major transcript expressed in these cells was composed of the vector-derived exon and the *Prnp* exon 3, similar to that in pPrPwild-transfected cells (Fig. 2A and B). This compositional similarity of the transcripts indicates that the pre-mRNAs expressed from pPrPwild and pPrP3′targeted are similarly processed in these transfected cells. Since pPrP3′targeted lacks the commonly targeted *Prnp* 3′ UTR, deletion of this part is unlikely to be involved in the

Fig. 1. (A) *Prnp* alleles in wild-type, Ngsk $Prnp^{0/0}$, Rcm0 $Prnp^{0/0}$, and Zrch II $Prnp^{0/0}$ mice. In Ngsk $Prnp^{0/0}$ mice, a 2.1-kb *Prnp* genomic DNA comprising 900-bp of intron 2, 10-bp of the 5′ UTR, an entire PrP ORF, and 450-bp of the 3′ UTR was replaced with a neomycin cassette (Sakaguchi et al., 1995). A similar part of *Prnp* was targeted in Rcm0 $Prnp^{0/0}$ mice (Moore et al., 1999). In Zrch II $Prnp^{0/0}$ mice, the *Prnp* genomic region consisting of 250-bp of intron 2, the entire exon 3, and 600-bp of the downstream intervening sequence was deleted (Rossi et al., 2001). Thus, 250-bp of intron 2 and a subsequent part of exon 3 including 10-bp of the 5′ UTR, the ORF, and 450-bp of the 3′ UTR are commonly targeted. (B) Schematic structures of the expression vectors, pPrPwild, pPrPtargeted, pPrP3′targeted, and pPrP5′targeted. pPrPwild was constructed by ligation of a PrP genomic fragment, including part of intron 2, exon 3, and the 3′ downstream sequence, and a PrPLP/Dpl genomic fragment including a part of intron 1, exon 2, intron 2, exon 3 and the 3′ downstream sequence in tandem under the control of the HCMV IE promoter. Each exon 3 contains a native poly(A) signal. The ORFs for PrP and PrPLP/Dpl are replaced with those for DsRed and EGFP, respectively. pPrPtargeted lacks the same part of *Prnp* as in the ataxic lines of $Prnp^{0/0}$ mice as indicated by the dotted square. pPrP3′targeted lacks 450-bp of the PrP 3′ UTR and pPrP5′targeted lacks 250-bp of intron 2 and 10-bp of the 5′ UTR. (C) Fluorescent microscopic photographs of mouse neuroblastoma N2a cells 48 h after transient transfection with pPrPwild, pPrPtargeted, pPrP3′targeted, and pPrP5′targeted.

abnormal regulation of *Prnd* in the ataxic lines of *Prnp*$^{0/0}$ mice. In contrast, pPrP5′targeted showed green EGFP fluorescence in the cells (Fig. 1B) and expressed the major transcript consisting of the vector-derived exon that was aberrantly spliced to the downstream *Prnd* exon 2 (Fig. 2A and B), similar to pPrPtargeted (Fig. 1B). These results indicate that our newly established *in vitro* transient transfection system is highly feasible to investigate the genetic mechanism of the abnormal expression of PrPLP/Dpl in the ataxic lines of *Prnp*$^{0/0}$ mice. pPrP5′targeted lacks 249-bp of intron 2 and 10-bp of the 5′ UTR. Thus, it is suggested that deletion of either 249-bp of intron 2 or 10-bp of the 5′ UTR or both in *Prnp* is responsible for the abnormal expression of downstream *Prnd* in the ataxic lines of *Prnp*$^{0/0}$ mice.

We further employed the *in vitro* system with several additional vectors, which were constructed by sequentially deleting 249-bp of intron 2 from the 5′ end. pPrPint2(-3) possesses only 3-bp of intron 2, including a splice acceptor of dinucleotides AG, and the subsequent 10-bp of the 5′ UTR (Fig. 3A). N2a cells transfected by this vector expressed EGFP, similar to those of pPrPtargeted and pPrP5′targeted (Fig. 3B), indicating that deletion of *Prnp* intron 2 is responsible for the abnormal expression of *Prnd*-coding exon in the transfected cells. In contrast, pPrPint2(-26) and pPrPint2(-50), containing 3′ 26- and 50-bp of intron 2, respectively, together with 10-bp of the 5′ UTR, exhibited DsRed signals in the cells (Fig. 3A and B). These results indicate that the unsuccessful cleavage/polyadenylation-mediated abnormal expression of *Prnd*-coding exon in the transfected cells is attributable to deletion of at least the 3′ 26-bp of *Prnp* intron 2. It is also suggested that lack of the same sequence in *Prnp* is responsible for the abnormal expression of PrPLP/Dpl in the ataxic lines of *Prnp*$^{0/0}$ mice.

3.3. The in vitro transient transfection system visualizes the functional disconnection of the pre-mRNA machineries underlying the abnormal expression of PrPLP/Dpl

Within the 26-bp intronic sequence, various elements important for pre-mRNA splicing, including a splice branch point, a polypyrimidine tract, and a splice acceptor are present. To investigate whether disruption of these elements could be involved in the impairment of pre-mRNA cleavage/polyadenylation at the end of *Prnp* leading to EGFP expression, we introduced various point mutations into the splice acceptor and/or the branch point in pPrPint2(-26). pPrPint2(-26)AG, carrying a G to T mutation in both the authentic splice acceptor AG and the adjacent downstream cryptic AG in the 5′ UTR, showed expression of EGFP in the cells (Fig. 4A and B). pPrPint2(-26)AGBr2× including mutations in all of these branch points and splice acceptors similarly expressed EGFP in the cells (Fig. 4A and B). These results clearly indicate that disruption of the splice acceptor in *Prnp* intron 2 caused expression of the downstream EGFP-coding exon. In contrast, pPrPint2(-26)Br carries an A to T mutation at the authentic branch point and expressed DsRed in the transfected N2a cells (Fig. 4A and B). Similar DsRed expression was observed in the cells transfected by pPrPint2(-26)Br2×, which contained an additional A to G mutation at the 2-bp downstream cryptic branch point (Fig. 4A and B). Therefore,

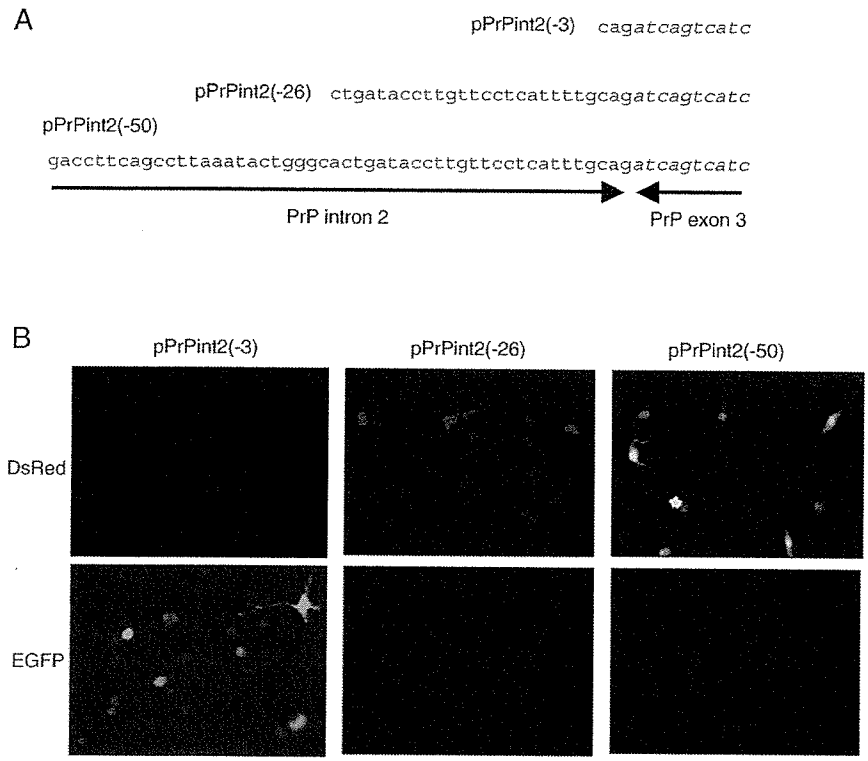

Fig. 3. (A) Nucleotide sequences of PrP intron 2 and exon 3 in pPrPint2(-3), pPrPint2(-26), and pPrPint2(-50). Italic letters are nucleotides in exon 3. (B) Fluorescent microscopic photographs of N2a cells 48 h after transient transfection with pPrPint2(-3), pPrPint2(-26), and pPrPint2(-50).

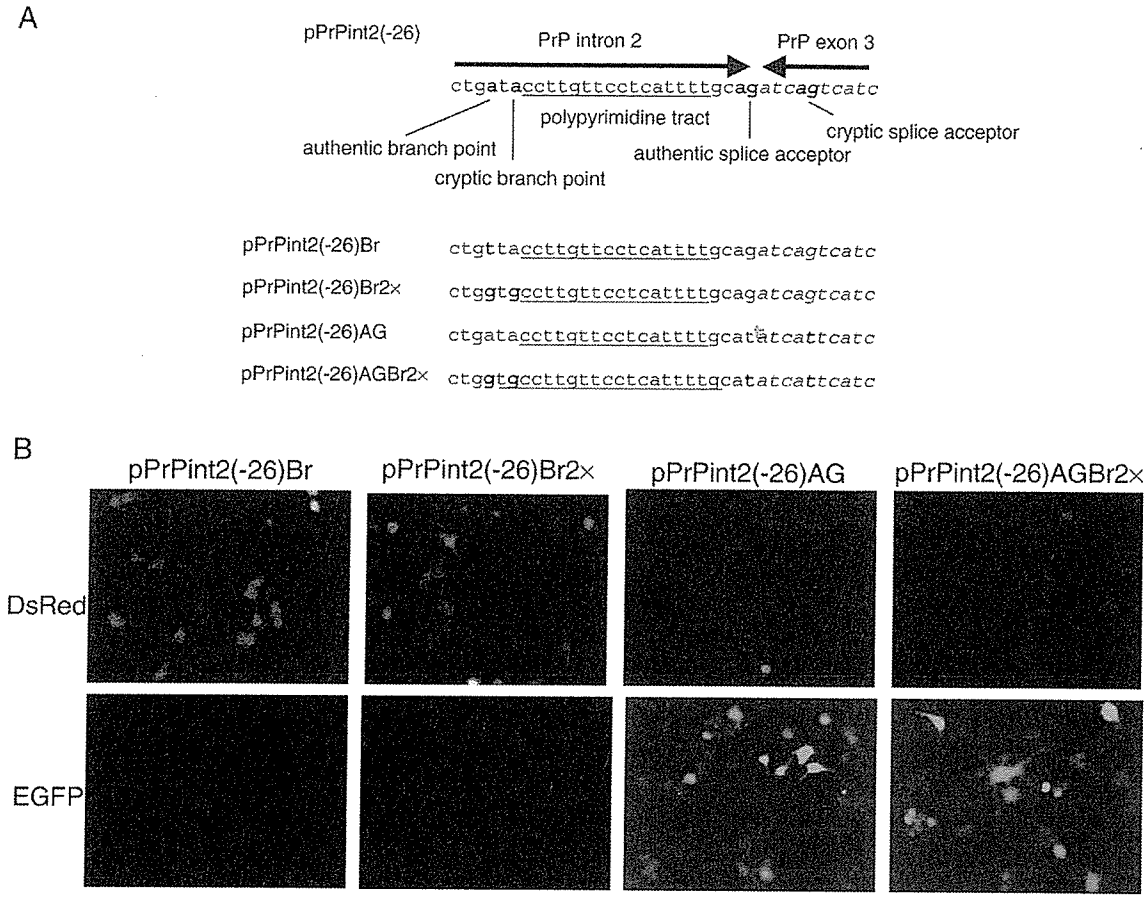

Fig. 4. (A) Point mutations introduced in the splice elements of pPrPint2(-26)Br, pPrPint2(-26)Br2×, pPrPint2(-26)AG, and pPrPint2(-26)AGBr2×. Nucleotide sequences in PrP intron 2 and exon 3 of pPrPint2(-26) are shown, including authentic and cryptic branch points, splice acceptors and a polypyrimidine tract. Mutated nucleotides are shown in bold letters. (B) Fluorescent microscopic photographs of N2a cells 48 h after transient transfection with pPrPint2(-26)Br, pPrPint2(-26)Br2×, pPrPint2(-26)AG, and pPrPint2(-26)AGBr2×.

it appears that lack of the functional branch point is unlikely to be involved in the abnormal expression of *Prnd*. However, pPrPint2(-3), which possesses the splice acceptor but lacks the branch point and polypyrimidine tract, expressed EGFP in N2a cells (Fig. 3B), indicating that deletion of the branch point or polypyrimidine tract might also be responsible for the expression of EGFP. It is thus possible that the expression of DsRed in the cells transfected by pPrPint2(-26)Br or pPrPint2(-26)Br2× is due to the presence of other functional cryptic branch points. Taken together, these results indicate that collapse in the integrity of splicing machineries could be responsible for the expression of EGFP in the cells by causing the impaired cleavage/polyadenylation of pre-mRNA. It is recently believed that splicing of the terminal intron is functionally linked to the cleavage/polyadenylation of pre-mRNA during transcription (Steinmetz, 1997; Proudfoot et al., 2002; Kornblihtt et al., 2004). It is therefore very likely that the functional disconnection of pre-mRNA machineries, in particular those of splicing and cleavage/polyadenylation, underlies the abnormal expression of PrPLP/Dpl in the ataxic lines of $Prnp^{0/0}$ mice. More importantly, these results indicate that our established *in vitro* transient transfection system is very useful to easily detect the functional disconnection of the pre-mRNA machineries from the expression of the EGFP fluorescent protein under fluorescence microscopy.

Splicing is mediated by a large molecular complex, splicesome, consisting of small nuclear ribonucleoproteins (snRNPs) and non-RNP splicing factors of a SR protein family (Proudfoot et al., 2002). The cleavage/polyadenylation of pre-mRNA is also regulated by various factors, including poly(A) polymerase (PAP), cleavage/polyadenylation specificity factor (CPSF), and cleavage stimulatory factor (Wahle and Ruegsegger, 1999; Proudfoot et al., 2002). U2AF is a dimeric splicing factor, interacting with the splice acceptor and polypyrimidine tract and helping recruit the U2 snRNP to the branch point together with a branch point binding protein (Vagner et al., 2000). It has been shown that PAP can interact with the large subunit of U2AF, U2AF65, and stimulate pre-mRNA splicing *in vivo* (Vagner et al., 2000). It was also reported that U2AF65 increased 3′-end cleavage efficiency (Millevoi et al., 2002). It is therefore conceivable that U2AF is a key molecule functionally connecting splicing and cleavage/polyadenylation. However, the molecular mechanism of how the pre-mRNA machineries are functionally connected to each other remains to be investigated.

Thus, our newly established *in vitro* transient transfection system might be employed to investigate the mechanism of the functional connection between the pre-mRNA machineries.

Recently, it has been shown that some viral proteins can disturb the function of pre-mRNA machineries by interacting with their components. Influenza virus NS1 protein was shown to inhibit cleavage/polyadenylation processes of cellular pre-mRNA by interacting with the 30 kDa subunit of CPSF (Nemeroff et al., 1998). Shimizu et al. subsequently reported that transcripts for the major heat shock protein HSP70, and β-actin were elongated due to the insufficient cleavage of these corresponding pre-mRNAs in influenza virus-infected cells (Shimizu et al., 1999). It was also shown that Epstein–Barr virus protein nuclear antigen 5 could inhibit cleavage/polyadenylation of cellular pre-mRNA (Dufva et al., 2002), and that human cytomegalovirus infection altered splicing and polyadenylation of cellular pre-mRNA (Adair et al., 2004). Interestingly, it was shown that Tgat, an oncogenic protein, was newly generated probably due to the impaired pre-mRNA processing in adult T-cell leukemia, the disease caused by human T-cell leukemia virus (Yoshizuka et al., 2004). Therefore, our newly established system may also be applied to elucidation of the molecular pathogenesis of pathological conditions.

3.4. Conclusions

In this study, we newly established an *in vitro* transient transfection system in which the functional disconnection of the pre-mRNA machineries could easily be detected by the expression of EGFP fluorescent protein under fluorescence microscopy. Employing this system, we showed that the abnormal expression of PrPLP/Dpl in ataxic lines of $Prnp^{0/0}$ mice can be visualized by expression of the green fluorescence protein EGFP in cultured cells, and identified that the abnormal expression of PrPLP/Dpl is probably due to functional disconnection between the pre-mRNA machineries, in particular those of splicing and cleavage/polyadenylation. Therefore, our newly established *in vitro* system might be useful to investigate the molecular mechanisms of the functional connection between the pre-mRNA machineries in normal and pathological conditions.

Acknowledgement

This study was supported in part by a Research on Specific Diseases grant from the Ministry of Health, Labour and Welfare, Japan.

References

Adair, R., Liebisch, G.W., Su, Y., Colberg-Poley, A.M., 2004. Alteration of cellular RNA splicing and polyadenylation machineries during productive human cytomegalovirus infection. J. Gen. Virol. 85, 3541–3553.

Anderson, L., Rossi, D., Linehan, J., Brandner, S., Weissmann, C., 2004. Transgene-driven expression of the Doppel protein in Purkinje cells causes Purkinje cell degeneration and motor impairment. Proc. Natl. Acad. Sci. U. S. A. 101, 3644–3649.

Behrens, A., et al., 2002. Absence of the prion protein homologue Doppel causes male sterility. EMBO J. 21, 3652–3658.

Bueler, H., et al., 1992. Normal development and behaviour of mice lacking the neuronal cell-surface PrP protein. Nature 356, 577–582.

Dufva, M., Flodin, J., Nerstedt, A., Ruetschi, U., Rymo, L., 2002. Epstein–Barr virus nuclear antigen 5 inhibits pre-mRNA cleavage and polyadenylation. Nucleic Acids Res. 30, 2131–2143.

Kornblihtt, A.R., de la Mata, M., Fededa, J.P., Munoz, M.J., Nogues, G., 2004. Multiple links between transcription and splicing. RNA 10, 1489–1498.

Li, A., et al., 2000a. Identification of a novel gene encoding a PrP-like protein expressed as chimeric transcripts fused to PrP exon 1/2 in ataxic mouse line with a disrupted PrP gene. Cell. Mol. Neurobiol. 20, 553–567.

Li, A., et al., 2000b. Physiological expression of the gene for PrP-like protein, PrPLP/Dpl, by brain endothelial cells and its ectopic expression in neurons of PrP-deficient mice ataxic due to Purkinje cell degeneration. Am. J. Pathol. 157, 1447–1452.

Manson, J.C., Clarke, A.R., Hooper, M.L., Aitchison, L., McConnell, I., Hope, J., 1994. 129/Ola mice carrying a null mutation in PrP that abolishes mRNA production are developmentally normal. Mol. Neurobiol. 8, 121–127.

Millevoi, S., Geraghty, F., Idowu, B., Tam, J.L., Antoniou, M., Vagner, S., 2002. A novel function for the U2AF 65 splicing factor in promoting pre-mRNA 3′-end processing. EMBO Rep. 3, 869–874.

Moore, R.C., et al., 1999. Ataxia in prion protein (PrP)-deficient mice is associated with upregulation of the novel PrP-like protein Doppel. J. Mol. Biol. 292, 797–817.

Moore, R.C., et al., 2001. Doppel-induced cerebellar degeneration in transgenic mice. Proc. Natl. Acad. Sci. U. S. A. 98, 15288–15293.

Nemeroff, M.E., Barabino, S.M., Li, Y., Keller, W., Krug, R.M., 1998. Influenza virus NS1 protein interacts with the cellular 30 kDa subunit of CPSF and inhibits 3′end formation of cellular pre-mRNAs. Mol. Cell 1, 991–1000.

Proudfoot, N.J., Furger, A., Dye, M.J., 2002. Integrating mRNA processing with transcription. Cell 108, 501–512.

Rossi, D., et al., 2001. Onset of ataxia and Purkinje cell loss in PrP null mice inversely correlated with Dpl level in brain. EMBO J. 20, 694–702.

Sakaguchi, S., et al., 1995. Accumulation of proteinase K-resistant prion protein (PrP) is restricted by the expression level of normal PrP in mice inoculated with a mouse-adapted strain of the Creutzfeldt–Jakob disease agent. J. Virol. 69, 7586–7592.

Sakaguchi, S., et al., 1996. Loss of cerebellar Purkinje cells in aged mice homozygous for a disrupted PrP gene. Nature 380, 528–531.

Shimizu, K., Iguchi, A., Gomyou, R., Ono, Y., 1999. Influenza virus inhibits cleavage of the HSP70 pre-mRNAs at the polyadenylation site. Virology 254, 213–219.

Steinmetz, E.J., 1997. Pre-mRNA processing and the CTD of RNA polymerase II: the tail that wags the dog? Cell 89, 491–494.

Vagner, S., Vagner, C., Mattaj, I.W., 2000. The carboxyl terminus of vertebrate poly(A) polymerase interacts with U2AF 65 to couple 3′-end processing and splicing. Genes Dev. 14, 403–413.

Wahle, E., Ruegsegger, U., 1999. 3′-End processing of pre-mRNA in eukaryotes. FEMS Microbiol. Rev. 23, 277–295.

Yamaguchi, N., Sakaguchi, S., Shigematsu, K., Okimura, N., Katamine, S., 2004. Doppel-induced Purkinje cell death is stoichiometrically abrogated by prion protein. Biochem. Biophys. Res. Commun. 319, 1247–1252.

Yoshizuka, N., et al., 2004. An alternative transcript derived from the trio locus encodes a guanosine nucleotide exchange factor with mouse cell-transforming potential. J. Biol. Chem. 279, 43998–44004.

Available online at www.sciencedirect.com
ScienceDirect
Vaccine 25 (2007) 985–992
Vaccine
www.elsevier.com/locate/vaccine

Immunization with recombinant bovine but not mouse prion protein delays the onset of disease in mice inoculated with a mouse-adapted prion

Daisuke Ishibashi [a], Hitoki Yamanaka [a], Naohiro Yamaguchi [b], Daisuke Yoshikawa [b], Risa Nakamura [b], Nobuhiko Okimura [b], Yoshitaka Yamaguchi [d], Kazuto Shigematsu [c], Shigeru Katamine [b], Suehiro Sakaguchi [a,b,d,*]

[a] *PRESTO Japan Science and Technology Agency, 4-1-8 Honcho Kawaguchi, Saitama, Japan*
[b] *Department of Molecular Microbiology and Immunology, Nagasaki University Graduate School of Biomedical Sciences, 1-12-4 Sakamoto, Nagasaki 852-8523, Japan*
[c] *Department of Pathology, Nagasaki University Graduate School of Biomedical Sciences, 1-12-4 Sakamoto, Nagasaki 852-8523, Japan*
[d] *Division of Molecular Cytology, The Institute for Enzyme Research, The University of Tokushima, 3-18-15 Kuramoto-cho, Tokushima 770-8503, Japan*

Received 26 June 2006; received in revised form 25 August 2006; accepted 26 September 2006
Available online 6 October 2006

Abstract

Host tolerance to endogenous prion protein (PrP) has hampered the development of prion vaccines as PrP is a major component of prions. Indeed, we show that immunization of mice with mouse recombinant PrP elicited no prophylactic effect against a mouse-adapted prion. However, interestingly, mice immunized with recombinant bovine PrP developed the disease significantly later than non-immunized mice after inoculation of a mouse prion. Sheep recombinant PrP exhibited variable prophylactic effects. Mouse recombinant PrP stimulated only very weak antibody responses. In contrast, bovine recombinant PrP was higher immunogenic and produced variable amounts of anti-mouse PrP autoantibodies. Sheep recombinant PrP was also immunogenic but produced more variable amounts of anti-PrP autoantibodies. These results might open a new way for development of prion vaccines.

Keywords: Prion; Vaccine; Tolerance

1. Introduction

Transmissible spongiform encephalopathies or prion diseases, including Creutzfeldt–Jakob disease (CJD) in humans and scrapie and bovine spongiform encephalopathy (BSE) in animals, are a group of devastating neurodegenerative disorders transmitted by unconventional infectious agents, the so-called prions [1,2]. Many lines of recent evidence suggest that BSE prions could orally transmit to humans via contaminated food, causing new variant type CJD in young people [3–5]. It was also recently reported that blood transfusion could be a risk factor for prion transmission in humans, causing subsequent CJD in recipients [6,7]. However, no prophylactic measures against the transmission of prions have been developed.

Prions are thought to be mainly composed of the proteinase K (PK)-resistant, amyloidogenic isoform of prion protein, designated PrP^{Sc}, which is generated by conformational conversion of the normal cellular isoform of PrP (PrP^{C}) via unknown post-translational modifications [1,2]. PrP^{C} is

* Corresponding author at: Division of Molecular Cytology, The Institute for Enzyme Research, The University of Tokushima, 3-18-15 Kuramoto-cho, Tokushima 770-8503, Japan. Tel.: +81 88 633 7438; fax: +81 88 633 7440.
E-mail address: sakaguch@ier.tokushima-u.ac.jp (S. Sakaguchi).

0264-410X/$ – see front matter © 2006 Elsevier Ltd. All rights reserved.
doi:10.1016/j.vaccine.2006.09.078

a glycosylphosphatidylinositol (GPI)-anchored membrane glycoprotein most abundantly expressed in neurons [1,2]. PrP is therefore a plausible target molecule for the development of prophylactic measures against prions. Gabizon et al. previously reported that polyclonal antibodies against PrP could reduce the infectivity of hamster-adapted prions by a factor of 100 [8]. Heppner et al. [9] recently showed that mice transgenically expressing anti-PrP monoclonal antibody, 6H4, were resistant to the disease after intraperitoneal inoculation of mouse-adapted scrapie RML prions. White et al. also demonstrated that two other anti-PrP monoclonal antibodies, ICSM 18 and 35 could prevent prion infection in mice by passive immunization [10]. This successful prevention of prion infection by anti-PrP antibodies indicates that active immunization or vaccination against PrP could be a promising prophylaxis against prion transmission.

In the present study, we immunized BALB/c mice with recombinant mouse, bovine, and sheep PrPs and thereafter intraperitoneally challenged these immunized mice with a mouse-adapted prion. Immunization with mouse recombinant PrP showed no prophylactic effect against the prion infection in mice. Instead, the immunization appeared to exacerbate the infection. In contrast, mice immunized with bovine recombinant PrP exhibited slightly but significantly prolonged incubation times, compared with those of non-immunized mice. The immunizing effects of sheep recombinant PrP on the infection were variable.

2. Materials and methods

2.1. Expression and purification of recombinant PrP immunogens

DNA fragments corresponding to the mouse PrP residues 23–231 (according to GenBank accession no. M13685), the sheep PrP residues 25–234 (GenBank accession no. U67922), and the bovine PrP residues 25–242 (GenBank accession no. AJ298878) were independently amplified by polymerase chain reaction (PCR) using appropriate primer pairs shown in Table 1. Following sequence confirmation of these PCR products, the fragments were digested with *Bam*HI and *Hin*dIII and inserted into a pQE30 vector (QIAGEN, Hilden, Germany). The pQE30 vector was developed to produce the proteins of interest with a N-terminal 6× His tag.

E. coli (M15) cells were freshly transformed by each plasmid, cultured in LB medium containing 1 mM isopropylthio-β-D-galactoside (IPTG), and collected by centrifugation. The collected cells were lysed using CelLytic B bacterial cell lysis/extraction reagent (Sigma–Aldrich Co., St. Louis, USA) in the presence of deoxyribonuclease I and the lysate was centrifuged at 25,000 × *g* for 10 min. The resulting pellet was suspended in Reagent containing 0.2 mg/ml lysozyme and incubated with occasional shaking at room temperature (RT) for 15 min. Volume of the suspension was then increased by addition of 1:10 diluted Reagent and centrifuged at 25,000 × *g* for 10 min. The resulting pellet was washed 3 times with the 1:10 diluted Reagent, suspended in a lysis buffer (8 M Urea, 10 mM Tris–HCl, 100 mM Na_2HPO_4, pH 8.0) and further purified using a Ni-NTA column (QIAGEN) as recommended in the manufacturer's protocol.

2.2. Purification of recombinant mouse PrP minus a 6× His tag

The DNA fragment corresponding to mouse PrP 23–231 was amplified by PCR using an appropriate pair of primers (Table 1). Following sequence confirmation, this fragment was digested with *Nde*I and *Bam*HI and inserted into a pET11a vector (Novagen, Inc., WI, USA). *E. coli* (BL21) cells were transformed by the resulting plasmid and cultured in LB medium containing 1 mM IPTG. The cells were collected by centrifugation and suspended in buffer (50 mM Tris–HCl, 1 mM EDTA, 100 mM NaCl, 1 mM PMSF, pH 8) containing 300 μg/ml lysozyme. After incubation for 20 min at RT, deoxycholic acid was added to the suspension for another 20 min and genomic DNA was digested with deoxyribonuclease I at RT for 30 min. The resulting extract was again centrifuged at 25,000 × *g* for 20 min and the pellet was solubilized in buffer (8 M urea, 50 mM Tris–HCl, 1 mM EDTA, pH 8). This extract was applied to a CM-sepharose column (Amersham Pharmacia Biotech AB, Uppsala, Sweden) and recombinant PrP was eluted using a linear NaCl gradient from 0 to 500 mM in the same buffer.

2.3. Immunization

Purified recombinant PrPs with a 6× His tag were dialyzed against PBS and 100 μg of each recombinant protein were intraperitoneally inoculated into a 4 week-old female

Table 1
The DNA sequences of primers used for constructs

Constructs	Forward primers	Reverse primers
6× His-tagged PrPs		
Mouse PrP23–231	gcggatccaaaaagcggccaaagcctggag	ccaagcttctatcagctggatcttctcccgtcgta
Bovine PrP25–242	gcggatccaagaagcgaccaaaacctggag	ccaagcttctatcaacttgcccctcgttggtaata
Sheep PrP25–234	gcggatccaagaagcgaccaaacctggcg	ccaagcttctatcaacttgccccctttggtaata
Non-tagged PrP		
Mouse PrP23–231	ggatgccatatgaaaaagcggccaaag	gaggatcctattagctggatcttctccc

Underlined sequences indicate appropriate restriction enzyme sites described in Section 2.

BALB/c mouse (SLC Japan, Shizuoka, Japan) at 2-week intervals together with complete Freund's adjuvant (Difco Laboratories, Detroit, MI) for the first immunization and with incomplete Freund's adjuvant (Difco Laboratories) from the second immunization. Antisera were collected 1 week after the final immunization and stored at −20 °C until used. Mice were cared for in accordance with the Guidelines for Animal Experimentation of Nagasaki University.

2.4. Prion inoculation

Brains were removed from the diseased mice infected with the mouse-adapted Fukuoka-1 prion [11] and homogenized to 1% (w/v) in PBS. Aliquots (100 μl) of the homogenate were intraperitoneally inoculated into each mouse 1 week after receiving their fifth immunization with recombinant PrPs.

2.5. Enzyme-linked immunosorbent assay (ELISA)

Each well of a 96-well immunoplate (Nunc) was coated with 500 ng of purified mouse recombinant PrP without a 6× His tag or other recombinant PrPs with a 6× His-tag by overnight incubation at 4 °C and then blocked with PBS containing 0.05% Tween-20 (T-PBS) and 25% Block Ace (Dainihonseiyaku Co., Tokyo, Japan) at 37 °C for 1 h. To detect specific IgG antibodies, serially 10-fold diluted antiserum was added to the wells for 1 h at 37 °C and unbound antibodies were removed by washing twice with T-PBS. Immune complexes were detected using secondary sheep anti-mouse IgG antibodies conjugated with HRP (Amersham Biosciences), 2 mM 2,2′-azino-bis(3-ethylbenzthiazoline-6-sulfonic acid), and 0.04% H_2O_2. Anti-PrP antibodies titers were determined using colorimetric values expressed at 405 nm.

For ELISA of mouse PrP peptides, moPrP90–109, moPrP131–154, and moPrP219–231, 1 μg of each peptide was coated on a 96-well immunoplate (Nunc) and similarly subjected to the procedures described above except for using 3,3′,5,5′-tetramentylbenzidine (Pierce, Rockford, IL) instead of 2 mM 2,2′-azino-bis(3-ethylbenzthiazoline-6-sulfonic acid) and detecting signals at 450 nm instead of 405 nm. The peptides (>70% purity) were purchased from Sigma–Aldrich Japan K.K. (Hokkaido, Japan).

2.6. Constructions of expression vectors for mouse, sheep, and bovine PrP^C

The DNA fragment encoding full-length mouse PrP^C was amplified by PCR with a sense primer (5′-tcggatcc-agtcatc**atg**gcgaaccttggc-3′; the underlined sequence, a *Bam*HI site; the bold sequence, a start codon) and an antisense primer (5′-cctctagacc**tca**tcccacgatcaggaaga-3′; the underlined sequence, a *Xba*I site; the bold sequence, a stop codon) using a cloned mouse genomic DNA as a template. The DNA fragments for sheep and bovine PrP^C were similarly amplified with a sense primer (5′-tcggatccagtcatc**atg**gtgaaaagccac-3′; the underlined sequence, a *Bam*HI site; the bold sequence, a start codon) and an antisense primer (5′-cctctagacc**cta**tcctactatgagaaaaa-3′; the underlined sequence, a *Xba*I site; the bold sequence, a stop codon) using a cloned bovine PrP cDNA and a cloned sheep PrP genomic DNA as a template, respectively. After confirmation of the DNA sequences, each DNA fragment was digested by *Ban*HI and *Xba*I and introduced into a pcDNA3.1 vector (Invitrogen, Carlsbad, CA).

2.7. Immunoblotting of eukaryotic PrP^C

African green monkey kidney COS-7 cells were transiently transfected by a pcDNA3.1 vector (Invitrogen) inserted with or without the DNA fragment encoding full-length mouse, sheep, and bovine PrP^C using lipofectamin 2000 (Invitrogen) and lysed in lysis buffer (1% Triton X-100, 1% sodium deoxycholate, 300 mM NaCl, 100 mM Tris–HCl, pH 7.5) 3 days after transfection. Proteins were separated by 12% SDS-PAGE and electrically transferred onto an immobilon-P membrane (Millipore, MA, USA). The membrane was incubated with 1:400-diluted antiserum raised against recombinant PrPs in BALB/c mice and secondary sheep anti-mouse IgG antibodies conjugated with HRP (Amersham Biosciences). Immune complexes were visualized using the ECL system (Amersham Biosciences).

2.8. Flow cytometry

Cells were harvested with PBS containing 0.2% EDTA, suspended in BSS buffer (140 mM NaCl, 5.4 mM KCl, 0.8 mM $MgSO_4$, 0.3 mM Na_2HPO_4, 0.4 mM KH_2PO_4, 1 mM $CaCl_2$ pH 7.0), and incubated with 100-fold diluted antisera for 30 min on ice. The treated cells were then washed three times with BSS buffer, reacted with FITC-conjugated goat anti-mouse IgG (H+L) (Chemicon International, CA, USA), and analyzed by FACScan (Becton Dickinson, NJ, USA).

2.9. Statistical analysis

Logrank test was used for analysis of the incubation times between mice immunized with and without recombinant PrPs. Colorimetric data from ELISA were subjected to one way ANOVA followed by Tukey–Kramer multiple comparison test.

3. Results

3.1. Different effects of immunization with recombinant mouse, sheep, and bovine PrPs on mouse-adapted prion in mice

We intraperitoneally immunized BALB/c mice with purified recombinant mouse, sheep, and bovine PrPs (100 μg/mouse) five times at 2-week intervals and intraperitoneally inoculated a mouse-adapted Fukuoka-1 prion into

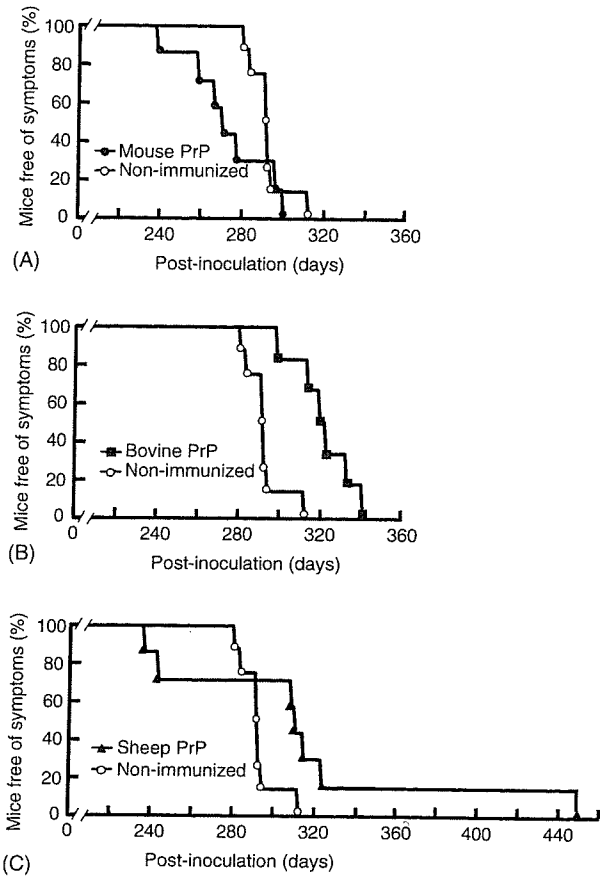

Fig. 1. Incubation times in mice immunized with mouse (A), bovine (B), and sheep (C) recombinant PrPs after intraperitoneal inoculation of a mouse-adapted Fukuoka-1 prion. (A) Incubation times in mice immunized with mouse recombinant PrP ($n=7$) and in non-immunized mice ($n=8$). No prophylactic effect from immunization with mouse recombinant PrP was detected. Instead, incubation times seemed to be shortened, compared with those of non-immunized mice. (B) Incubation times in mice immunized with bovine recombinant PrP ($n=6$) and in non-immunized mice ($n=8$). The immunized mice developed the disease with significantly delayed onset ($p=0.0008$, Logrank test). (C) Incubation times in mice immunized with sheep recombinant PrP ($n=7$) and in non-immunized mice ($n=8$). Except for two of the immunized mice, the other five mice showed extended incubation times compared to non-immunized mice.

the immunized mice 1 week after the final immunization. Non-immunized BALB/c mice developed the disease 291 ± 10 days post-inoculation (p.i.) (Fig. 1). Immunization with mouse recombinant PrP had no prophylactic effect against the disease. The immunized-mice succumbed to the disease at 269 ± 22 days p.i. (Fig. 1A). No significant difference in the incubation times could be detected between the mice immunized with and without mouse recombinant PrP ($p=0.22$, Logrank test), but incubation times of the immunized mice appeared to be shortened compared with those of the non-immunized mice. In contrast, mice immunized with recombinant bovine PrP showed significantly delayed onsets at 322 ± 15 days p.i., compared with non-immunized mice ($p=0.0008$, Logrank test, Fig. 1B). Immunization with recombinant sheep PrP showed variable effects against the prion. Five out of seven immunized mice developed the disease with prolonged onset (Fig. 1C). Two remaining mice became sick at 239 and 246 days p.i., as early as mice immunized with mouse recombinant PrP began to succumb (Fig. 1C). Accumulation of PrP^{Sc} and pathological changes including vacuolation and gliosis were indistinguishable in the brains of terminally diseased mice (data not shown).

3.2. Bovine and sheep but not mouse recombinant PrP stimulates antibody responses against respective immunogens in mice

To assess the immunogenicity of recombinant bovine, sheep, and mouse PrPs in mice, we investigated antibody responses in the immunized mice. Antisera were collected just before prion infection and each serum of the four to five immunized mice of each group was subjected to an ELISA to detect specific IgG antibodies against respective immunizing recombinant PrPs. In the mice immunized with mouse recombinant PrP, only slightly higher antibody binding expressed as optical density values at 405 nm (OD_{405}) were detected, compared with those of non-immunized mice (Fig. 2A). In contrast, much higher OD_{405} values were observed in the mice immunized with recombinant bovine and sheep PrPs (Fig. 2A). We also performed Western blotting of COS-7 cells transiently expressing mouse, sheep, and bovine PrP^C without a 6× His tag using the antisera. No mouse PrP^C could be detected by the anti-mouse recombinant PrP sera on Western blotting (Fig. 2B). In contrast, all of the anti-sheep and -bovine recombinant PrP sera we used for Western blotting substantially detected sheep and bovine PrP^C expressed in COS-7 cells, respectively (Fig. 2B). However, the signals were variable in intensity with each anti-sheep or -bovine recombinant PrP serum. Three out of four anti-bovine PrP sera showed relatively strong signals of bovine PrP^C but the remaining one exhibited faint signals (Fig. 2B). In the case of anti-sheep PrP sera, one antiserum revealed relatively strong signals but the remaining ones exhibited weak signals (Fig. 2B). These results indicate that recombinant bovine and sheep but not mouse PrP were immunogenic but their immunogenicities were variable in BALB/c mice.

We further carried out fluorescence activated cell sorter (FACS) analyses and found that the antisera against bovine and sheep PrPs also contained various amounts of antibodies capable of reacting with respective native PrP^C transiently expressed on COS-7 cells (Fig. 2C).

3.3. Anti-PrP autoantibodies are variably produced in mice immunized with recombinant bovine and sheep PrPs

We investigated whether the antisera against recombinant bovine and sheep PrPs could crossreact with mouse PrP by carrying out ELISA. The immunizing recombinant PrPs contained a 6× His tag. Therefore, to eliminate immunoreactivity

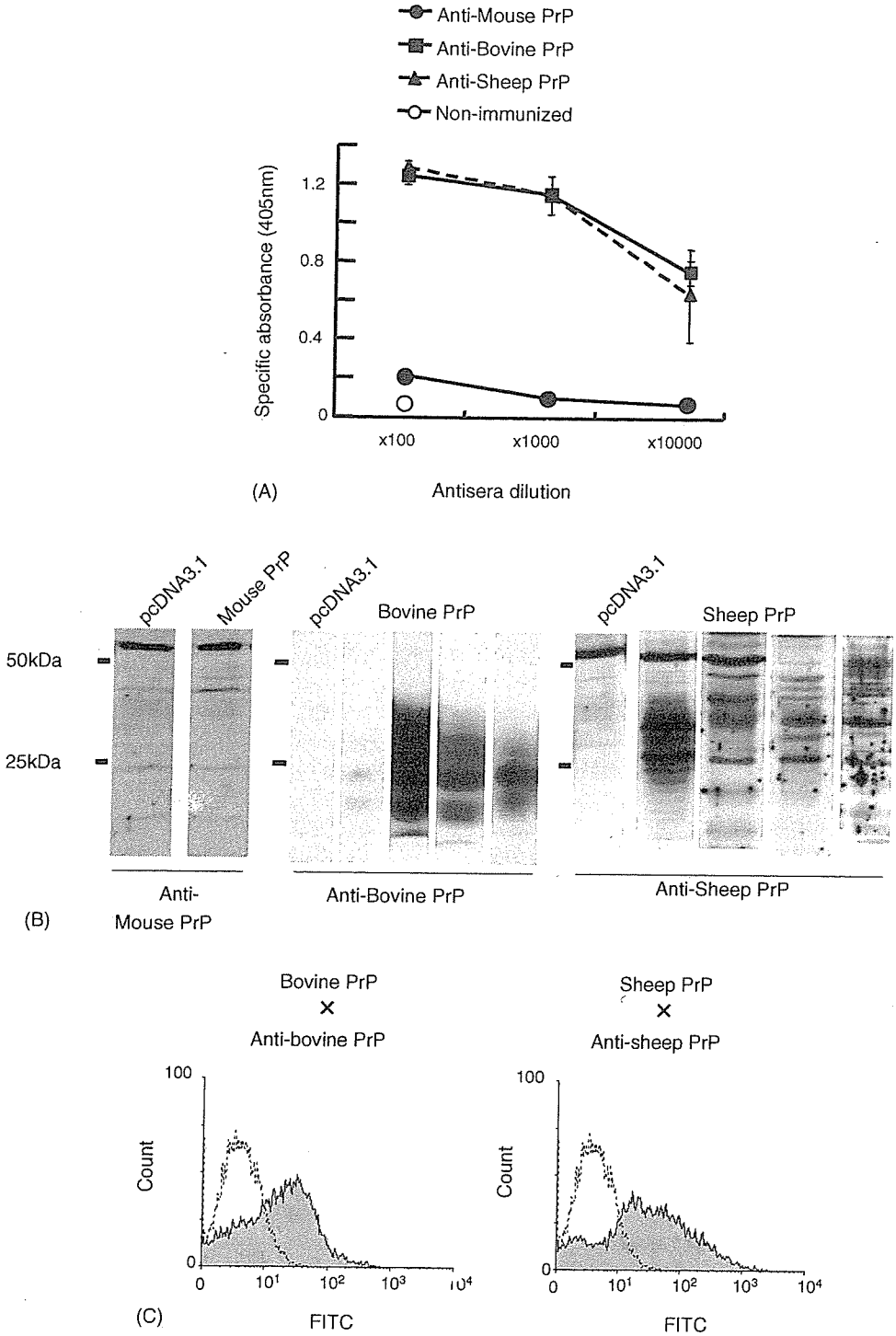

Fig. 2. Antibody responses in mice immunized with mouse, bovine, and sheep recombinant PrPs against the respective immunogens. (A) Each group of at least five mice was intraperitoneally immunized with the purified recombinant PrPs five times at 2-week intervals and anti-PrP IgG antibodies were detected in each serum of the immunized four to five mice of each group by an ELISA against the immunizing antigens. For anti-mouse PrP antibody detection, purified mouse recombinant PrP without a 6× His tag was used instead. (B) Antigenic specificities of each antiserum of the four immunized mice from each bovine and sheep recombinant PrP group were also examined by Western blotting of COS-7 cells transiently transfected with pcDNA3.1 vector alone or with pcDNA3.1 encoding each PrP^C. (C) FACS analysis of COS-7 cells transiently expressing each PrP^C. The cells transfected with the vector alone (unshaded) and the vector encoding bovine or sheep PrP^C (shaded) were probed by each antiserum.